Mater Renew Sustain Energy (2016) 5:7
DOI 10.1007/s40243-016-0071-3

ORIGINAL PAPER

Understanding the hydrogen storage behavior of promising Al–Mg–Na compositions using thermodynamic modeling

S. Abdessameud[1] · M. Medraj[1,2]

Received: 4 August 2015 / Accepted: 9 March 2016 / Published online: 5 April 2016

Abstract Thermodynamic modeling of the Al–Mg–Na–H system is performed in this work to understand the phase relationships and reaction mechanisms in this system. The Al–Na system is reassessed using the modified quasi-chemical model for the liquid phase. All the terminal solid solutions were remodeled using the compound energy formalism. The thermodynamic properties of the ternary systems are estimated from the models of the binary systems and the ternary compound using the CALPHAD method. The reaction pathways for the systems MgH_2/AlH_3, MgH_2/$NaAlH_4$, and MgH_2/Na_3AlH_6 are calculated and compared to the experimental data from the literature. Details about the reaction mechanisms and temperatures, the amount of the products, and their composition are revealed and discussed in this work. The calculations show that in the composites MgH_2/$NaAlH_4$ and MgH_2/Na_3AlH_6, the components spontaneously destabilize mutually in specific relative amounts by forming $NaMgH_3$, which may play only a catalytic role on the decomposition of (MgH_2 + Al) mixture, $NaAlH_4$, or Na_3AlH_6. Also, Al destabilizes MgH_2 and $NaMgH_3$ by forming β phase and reducing the decomposition temperatures of these hydrides by more than 50 °C. The constructed database is successfully used to reproduce the pressure–composition isotherms (PCIs) for Mg-10 at% Al and Mg-4 at% Al alloys at 350 °C. The results provide a better understanding of the reaction mechanisms in the PCIs found in the literature concerning the number of plateau pressures and their sloping. It is shown that the first plateau pressure observed during the PCIs of Al–Mg alloys depends on Al content and is higher than that of pure Mg. This difference is due to Al solubility in hcp-Mg.

Keywords Hydrogen storage · Magnesium hydrides · Sodium alanates · Thermodynamic modeling

Introduction

Hydrogen storage in light metal hydrides is considered as one of the most promising solutions toward a hydrogen economy. Lots of efforts have been devoted in the last few decades to the search of a metal hydride that satisfies all the requirements for the development of hydrogen fuel cells, with potential applications ranging from micro-fuel cells that power portable electronics to mobile applications. Magnesium hydride (MgH_2) shows a great potential as a hydrogen storage material because of its high hydrogen storage capacities (7.6 wt%), reversibility, and low cost [1]. However, it suffers from extremely slow hydriding kinetics and high decomposition temperature [1]. MgH_2 is predicted to decompose to hcp-Mg and H_2 at a temperature of 284.73 °C and ambient pressure [2]. Many studies have shown the possibility of lowering the decomposition temperature of MgH_2 and/or improving its hydriding kinetics by mixing with other elements or compounds. Another group of complex metal hydrides, alanates (or alumino-hydrides, a family of complex hydrides containing aluminum and hydrogen), have attracted great interest since the work of Bogdanovic [3] who demonstrated the

✉ M. Medraj
mmedraj@encs.concordia.ca

[1] Department of Mechanical Engineering, Concordia University, 1455 de Maisonneuve Blvd West, Montreal, QC H3G 1M8, Canada

[2] Department of Mechanical and Materials Engineering, Masdar Institute of Science and Technology, Masdar City, Abu Dhabi, United Arab Emirates

Table 1 Optimized model parameters for the different phases in the Al–Mg-Na–H system (J/mole)

Liquid phase (MQM)	
$g^0_{H(l)} = 74,266.7 - 26.2456T + 20.7856T\ln T$	[15]
$Z^{Mg}_{MgH} = Z^{H}_{MgH} = 6,\ \Delta g^0_{MgH} = -18,049.78$	
$Z^{Na}_{NaH} = Z^{H}_{NaH} = 6,\ \Delta g^0_{NaH} = -39,245.92 + 8.45T;$	[2]
$\Delta g^{10}_{NaH} = 12,133.6 - 0.711T;\ \Delta g^{01}_{NaH} = -66,944 + 8.368T$	
$Z^{Mg}_{MgNa} = 4.5,\ Z^{Na}_{MgNa} = 6,\ \Delta g^0_{MgNa} = 7,660.0 + 2.9T$	
$Z^{Al}_{AlH} = Z^{H}_{AlH} = 6,\ \Delta g^0_{AlH} = -6,516.58 - 0.544T$	[15]
$Z^{Mg}_{MgAl} = Z^{Al}_{MgAl} = 6,\ \Delta g^0_{MgAl} = -2761.44 + 1.52716T;\ \Delta g^{10}_{AgAl} = 481.4 + 0.6276T$	
$Z^{Al}_{AlNa} = Z^{Na}_{AlNa} = 6,\ \Delta g^0_{AlNa} = 203509.76 + 5.89944T;\ \Delta g^{10}_{AlNa} = -193133.44$	This work
Terminal solid solutions (compound energy formalism)	
hcp-(Mg) (Mg, Na, Al)$_2$(H, Va)$_1$	
${}^0G^{Mg_2}_{Mg.Va} = 2G(Mg_{hcp});{}^0G^{Na_2}_{Na.Va} = 2G(Na_{hcp});{}^0G^{Al_2}_{Al.Va} = 2G(Al_{hcp})$	[2]
${}^0G^{Mg_2H}_{Mg.H} = 173,217.6 - 242.672T + 2G(Mg_{hcp}) + 1/2(H_2, gas)$	
${}^0G^{Na_2H}_{Na.H} = 2G(Na_{hcp}) + 1/2G(H_2, gas);{}^0G^{Al_2H}_{Al:H} = 100000 + 2G(Al_{hcp}) + 1/2(H_2,\ gas)$	
${}^0L^{hcp}_{Mg,Na:Va} = 79,496 + 16.736T$	
${}^0L^{hcp}_{Mg,Al:Va} = 8288.059 - 8.75T;{}^1L^{hcp}_{Mg,Al:Va} = 414.886 - 6.109T;{}^0L^{hcp}_{Al,Na:Va} = 75132$	This work
bcc-(Na) (Na, Mg, Al)$_1$(H,Va)$_3$	
${}^0G^{NaH_3}_{Na:H} = G(Na_{bcc}) + 3/2G(H_2, gas);{}^0G^{MgH_3}_{Mg:H} = G(Mg_{bcc}) + 3/2G(H_2, gas);$	[2]
${}^0G^{AlH_3}_{Al:H} = G(Al_{bcc}) + 3/2G(H_2, gas)$	
${}^0G^{Na}_{Na:Va} = G(Na_{bcc});{}^0G^{Mg}_{Mg:Va} = G(Mg_{bcc});{}^0G^{Al}_{Al:Va} = G(Al_{bcc})$	
${}^0L^{bcc}_{Na:H,Va} = -5,569.8;{}^1L^{bcc}_{Na:H,Va} = -2,092.9;;{}^0L^{bcc}_{Na,Mg:Va} = 30,000$	
${}^0L^{bcc}_{Al,Na:Va} = 27715$	[13]
${}^0L^{bcc}_{Al,Mg:Va} = 5020.8$	[14]
fcc-Al (Al, Mg, Na)$_1$(H, Va)$_1$	
${}^0G^{Al}_{Al:Va} = G(Al_{fcc});{}^0G^{Mg}_{Mg:Va} = G(Mg_{fcc});{}^0G^{Na}_{Na:Va} = G(Na_{fcc});$	
${}^0G^{AlH}_{Al:H} = G(Al_{fcc}) + 1/2G(H_2, gas) + 100000;{}^0G^{NaH}_{Na:H} = G(Na_{fcc}) + 1/2G(H_2, gas) + 130T$	[13]
${}^0L^{fcc}_{Al:H,Va} = -45,805 + 56.43T$	
${}^0G^{MgH}_{Mg:H} = G(Mg_{fcc}) + 1/2G(H_2, gas) + 100000$	This work
${}^0L^{fcc}_{Al:Mg,Va} = 3349.069 - 1.6763T;{}^1L^{fcc}_{Mg:Al,Va} = 169.787 - 3.05459T;{}^0L^{fcc}_{Al:Na,Va} = 77741.6;{}^0L^{fcc}_{Mg,Na:Va} = 20000$	
Nonstoichiometric compounds [14]	
$\gamma(Al_{12}Mg_{17}) : (Mg)_{10}(Al, Mg)_{24}(Al, Mg)_{24}$:	
$G^{\gamma}_{Mg:Al:Al} = 10G(Mg_{hcp}) + 48G(Al_{fcc}) + 178762.96 - 203T;G^{\gamma}_{Mg:Mg:Al} = 34G(Mg_{hcp}) + 24G(Al_{fcc}) - 208742 + 78.474T$	
$G^{\gamma}_{Mg:Al:Mg} = 34G(Mg_{hcp}) + 24G(Al_{hcp}) + 359507.2 - 197.664T;G^{\gamma}_{Mg:Mg:Mg} = 58G(Mg_{hcp}) + 359153.4 - 174.58T$	
$\beta(A_3Mg_2) : (Al)_{19}(Al, Mg)_2(Mg)_{12}$	
$G^{\beta}_{Al:Al:Mg} = 12G(Mg_{hcp}) + 21G(Al_{fcc}) - 82110.6 - 13.8072T;G^{\beta}_{Al:Mg:Mg} = 14G(Mg_{hcp}) + 19G(Al_{fcc}) - 72445.56 - 27.6144T$	
Stoichiometric compounds	
MgH_2: $G^0_{MgH_2} = -82,842.15 + 25.42T - 2.87T\ln T - 55.30 \times 10^{-3}T^2 - 34,305.5T^{-1}$	[1]
NaH: $G^0_{NaH} = -75,767.99 + 293.72T - 48.69T\ln T - 0.26 \times 10^{-3}T^2 + 1.80 \times 10^{-8}T^3 + 632,658.0T^{-1}$	[2]
$NaMgH_3$:	
$G_{NaMgH_3} = -157,905.82 + 185.83T - 33.6T\ln T - 61.27 \times 10^{-3}T^2$	[2]
AlH_3: $G_{AlH_3} = -28,415 + 213.712933T - 41.75632T\ln T - 14.548469 \times 10^{-3}T^2 + 446400T^{-1}$	[13]
ε ($Al_{30}Mg_{23}$): $G_{\varepsilon} = 23G(Mg_{hcp}) + 30G(Al_{fcc}) - 116327.71 + 1673.42T$	[14]
Al_2Li_3: $G_{Al_2Li_3} = 2G(Al_{fcc}) + 3G(Li_{bcc}) - 89,690 + 33.96T$	This work
Al_4Li_9: $G_{Al_4Li_9} = 4G(Al_{fcc}) + 9G(Li_{bcc}) - 438,967.89 + 69.28T$	This work

reversibility of the hydrogenation of the Ti-enhanced alanates. Sodium alanate, $NaAlH_4$, decomposes in two steps with total hydrogen release of 5.6 wt%. According to Qiu et al. [4], it is predicted that, at 1 bar, the first step proceeds at 21.45 °C and the second one at 106.58 °C. However, research is still needed to improve alanates absorption/desorption kinetics. Recently, great efforts have been made to investigate hydrogen storage properties and reaction mechanisms in composites containing MgH_2 and some complex hydrides such as magnesium and sodium alanates where different explanations have been given about the observed processes [5–11]. However, no theoretical work has been conducted to better understand these experimental results.

In the present work, thermodynamic modeling is used to construct a self-consistent thermodynamic database that describes the Al–Mg–Na–H system and allows the prediction of its hydrogen storage performance and provides a basic understanding of the reaction mechanisms between the different phases in the system under equilibrium conditions. Recently, Abdessameud et al. [2] performed thermodynamic modeling of the Mg–Na–H system and predicted its hydrogen storage properties over a wide range of temperatures and pressures. They [2] proved that the $MgNaH_3$ hydride does not affect the thermodynamics of MgH_2 and provided the best working conditions to benefit from its full catalytic role.

Literature review

This section is composed of two main parts. In the first part, a literature review about the thermodynamic properties and descriptions of the constituent binaries and ternaries in the Al–Mg–Na–H system is presented. In the second part, the most recent findings about the hydrogen storage properties in the Al–Mg–H and Al–Mg–Na–H systems are reviewed.

Thermodynamic description of the Al–Mg–Na–H system

The Al–Mg–Na–H system is modeled in the current work using FactSage software [12]. The constituent binary systems are modeled using the modified quasichemical model MQM for the liquid phase and the compound energy formalism for the solid solution phases. These binary systems are either taken from the literature [13–15] or from our previous work [2] or reassessed in the current work (Al–Na). In many occasions, the models found in the literature were adjusted to suit dealing with hydrogen. This will be elaborated in the following sections. The thermodynamic properties of the ternary systems are estimated from the models of the binary systems and the ternary compounds using the CALPHAD method.

Mg–Na–H system was reviewed and modeled for the first time in our previous work [2]. The constituent binaries (Mg–Na, Mg–H, and Na–H) were remodeled using the MQM for the liquid phase and three hydrides, MgH_2, NaH, and $MgNaH_3$, were described in this system [2]. The model parameters taken from [2] are used in this work.

The Al–Mg system

The model parameters used to describe the liquid phase of the Al–Mg system are from Harvey [14] who used the MQM to model this phase. In [14], the terminal solid solutions were considered substitutional. Since this system is used for hydrogen storage purposes, the terminal solid solutions are considered interstitial and are adjusted in this work. For the compounds, all the parameters used in [14] are adopted in this work. The phase diagram consists of a liquid phase, terminal fcc-Al and hcp-Mg solid solutions, and three compounds $\beta(Al_3Mg_2)$, $\gamma(Al_{12}Mg_{17})$, and $\varepsilon(Al_{30}Mg_{23})$.

The Al–H system

San-Martin and Manchester [16] conducted a critical literature review and assessment of the Al–H system. Three stable phases have been reported in the system: liquid, fcc-Al solid solution, and gas. They [16] reported a eutectic-type reaction near the melting point of Al (660.452 °C) and hydrogen solubilities of 1.1×10^{-3} and 1.16×10^{-4} at% in liquid Al and fcc-Al, respectively. Only one hydride, AlH_3, was reported in the literature [17]. AlH_3 has a gravimetric density that exceeds 10 wt% and shows rapid dehydrogenation at low temperatures (<100 °C) with a low heat of reaction (around −7 kJ/molH_2) which makes it a promising hydrogen storage material [17]. According to its thermodynamic properties, AlH_3 is metastable at ambient conditions, but its decomposition reaction suffers from poor kinetics [17]. Thus, after the first dehydrogenation, the resulting Al could be hydrogenated only at high pressure (106 MPa) and AlH_3 will not take part in the following hydrogenation/dehydrogenation cycles. Graetz et al. [17] published an extensive review about aluminum hydride as "a hydrogen and energy storage material". Qiu et al. [13] reviewed the existing thermodynamic properties of the Al–H system and modeled it. The calculations made by Qiu et al. [13] showed good agreement with experimental data for hydrogen solubility in fcc-Al and thermodynamic properties of AlH_3. Later, thermodynamic modeling of hydrogen solubility in liquid Al was conducted by Harvey and Chartrand [15] using the MQM, showing better agreement with the available experimental data. Since

MQM is used to describe the liquid phase in this work, the model parameters of Harvey and Chartrand [15] are used to describe the liquid phase in the present work. The model parameters given by Qiu et al. [13] for the AlH3 hydride and fcc-Al phase are also adopted in this work.

The Al–Na system

The Al–Na system has been extensively reviewed by Murray [18] and Zhang et al. [19]. The Al–Na system has been assessed by Murray [18], Zhang et al. [19], and Qiu et al. [13].

The assessed phase diagram by Murray [18] shows a miscibility gap in the liquid phase, low solubility of Na in fcc-Al and of Al in bcc-Na, and a monotectic reaction: Liquid 1 → Liquid 2 + fcc-Al at Na composition of 0.18 ± 0.02 at%.

Because different models are used in this study for the liquid phase (MQM) and for the terminal solid solutions than previous assessments [13, 18, 19], the system is reassessed in the present work. Scheuber et al. [20] conducted solubility measurements of Na in liquid Al by heating under hydrogen gas and quenching. It should be noted that their results are uncertain due to hydrogen contamination as pointed out by Murray [18]. Fink et al. [21] carried out direct and differential thermal analysis measurement to investigate Al liquidus and monotectic reaction in addition to electrical resistivity and metallographic measurements to investigate the Na solubility in solid Al. They [21] reported a monotectic composition and temperature of 0.18 at% Na and 932 K in addition to a maximum solubility of Na in fcc-Al of less than 0.003 at%. Two years later, Ransley and Neufeld [22] reported a lower value for the monotectic composition (0.14 at% Na occurring at 932 K) and more precise value of Na solubility in solid Al (0.0023 at% Na). Later, Na solubility in liquid Al measurements conducted by Hensen et al. [23] showed higher values compared to [20–22] and also increasing Na solubility with decreasing temperature. Two years later, Fellner et al. [24] reported saturated solubility data (of Na in liquid Al) close to the results of [20–22]. The activity of Na in molten Al was determined by Dewing [25] at 1293 and 1353 K and by Brisley and Fray for super purity Al [26] at 998 K. These data [25, 26] are used in the present work.

The Al–Mg–H system

Rokhlin and Ivanchenko [27] conducted a literature review on the Al–Mg–H system. Harvey et al. [14, 15] reviewed the hydrogen solubility experimental data of Al–Mg liquid alloys and used them in assessing this system using the MQM. These authors [14, 15] obtained good agreement with the experimental data from the literature [28–32]. Therefore, their model parameters of the Al–Mg–H liquid are adopted in this work. In the present work, the solubility of hydrogen in Al–Mg compounds [$\beta(Al_3Mg_2)$, $\gamma(Al_{12}Mg_{17})$ and $\varepsilon(Al_{30}Mg_{23})$] is neglected, because no significant experimental evidence exists for hydrogen solubility in these compounds in the literature [33, 34].

Only one metastable ternary compound, $Mg(AlH_4)_2$ (with P-3m1 structure and a gravimetric density of 9.3 wt%), has been reported in the literature [27]. Palumbo et al. [34] investigated the Al–Mg–H system using thermodynamic modeling and ab initio calculations. However, they [34] focused their literature review on magnesium alanate $Mg(AlH_4)_2$. Thermodynamic description of the $Mg(AlH_4)_2$ compound has been provided later by Grove et al. [35] and their parameters are used as initial values in the present work.

Decomposition of $Mg(AlH_4)_2$ has been investigated by different authors such as Mamatha et al. [36] and Varin et al. [37] using DSC and Kim et al. [38] using TG/MS and DSC, and Iosub et al. [39] using XRD, TPD (temperature programmed desorption), and DSC. It has been concluded that magnesium alanate, $Mg(AlH_4)_2$, decomposes in two steps [38, 40] according to the reactions:

$$Mg(AlH_4)_2 \rightarrow MgH_2 + 2Al + 3H_2\,(7\ \text{wt\%}\ H_2), \quad (1)$$

$$MgH_2 + 2Al \rightarrow 1/2\beta + 1/2Al + H_2\,(2.3\ \text{wt\%}\ H_2). \quad (2)$$

An enthalpy value of 1.7 kJ/mole for reaction 1 has been found by Mamatha et al. [36], while Varin et al. [37] reported a value close to zero. Iosub et al. [39] estimated that the enthalpy of reaction 1 approached 2 kJ/mol.

The Al–Mg–Na system

No experimental thermodynamic data and no ternary compound have been reported in the literature for the Al–Mg–Na system. Thermodynamic modeling of the system was performed by Zhang et al. [19] by combining the constituent binaries. Since MQM is used in this work, thermodynamic description of the system is predicted from extrapolation of the binaries cited in the "Al–Mg system" and "Al–Na system" (Al–Mg and Al–Na) and those assessed in our previous paper (Mg–Na) [2].

The Al–Na–H system

The Al–Na–H system has been reviewed and modeled by Qiu et al. [4]. Two ternary compounds have been reported in the literature [4], $NaAlH_4$ (with a tetragonal I41/a structure) and Na_3AlH_6 which exist in two forms: α-Na_3AlH_6 at temperatures lower than 252 °C (with a

monoclinic P21/c structure) and β-Na_3AlH_6 at temperatures higher than 252 °C (with cubic Fm-3m structure). $NaAlH_4$ decomposes in two steps as follows:

$$NaAlH_4 \rightarrow 1/3\alpha - Na_3AlH_6 + 2/3Al + H_2\,(3.7\ \text{wt\%}\ H_2), \quad (3)$$

$$\alpha - Na_3AlH_6 \rightarrow 3NaH + Al + 3/2H_2\,(1.9\ \text{wt\%}\ H_2). \quad (4)$$

Using the substitutional solution model, Qiu et al. [4] provided a thermodynamic description of the Al–Na–H liquid. They assessed the two compounds in the system using the CALPHAD approach and first principle calculations. Their parameters [4] are used in this work for the compounds. However, since the MQM is used in the present work, the ternary liquid has been extrapolated from the constituent binaries described in "Thermodynamic description of Al–Mg–Na–H system".

Hydrogen storage behavior in the Al–Mg–Na–H system

The Al–Mg–H system

Recently, Liu et al. [41] investigated the decomposition reaction of $Mg(AlH_4)_2$ using TPD, DSC, and XRD. They [41] reported that, after the first exothermic peak, two dehydrogenation overlapping endothermic peaks were observed. XRD measurements at 200, 280, and 320 °C showed that diffraction peaks of Al shifted toward lower angles indicating the increase of solubility of Mg in the Al phase. According to these authors [41], the overall dehydrogenation reaction proceeds as follows (with the first reaction as exothermic):

$$Mg(AlH_4)_2 \xrightarrow{125\text{-}200^\circ C} MgH_2 + 2\,Al + 3\,H_2 \xrightarrow{250\text{-}320^\circ C} 7/9\,MgH_2 + 20/9\,Al_{0.9}Mg_{0.1} + 29/9\,H_2 \xrightarrow{320\text{-}440^\circ C} 6/9\,Al_{0.9}Mg_{0.1} + 7/15\,Al_3Mg_2 + 4\,H_2 \quad (5)$$

In these equations, Liu et al. [41] referred to fcc-Al as $Al_{0.9}Mg_{0.1}$ by taking into account the value of the maximum solubility of Mg in fcc-Al at 320 °C as 10 at%. After recharging at 120–210 °C and 100 bar of hydrogen pressure, only MgH_2 and Al were formed [41].

The hydrogenation properties of Al–Mg alloys have been widely investigated [5, 6, 10, 11, 42–45]. It has been found [42, 43] that β (Al_3Mg_2) and γ ($Al_{12}Mg_{17}$) phases can be hydrogenated reversibly to form (MgH_2 + Al) and (MgH_2 + β), respectively.

Shang et al. [45] showed that the de-hydrogenation of MgH_2 is improved when mixed with Al using mechanical alloying. Zaluska et al. [44] suggested that Al is involved in hydriding/de-hydriding reactions through the reaction:

$$nMgH_2 + mAl \rightarrow Mg_nAl_m + nH_2. \quad (6)$$

Andreasen [46] reviewed the hydrogen storage properties of Al–Mg alloys and reported that the Mg_nAl_m compound (in reaction (6)) has been found to be mainly the β-phase.

Liu et al. [10] investigated the effect of Al on MgH_2 destabilization by ball milling mixtures of MgH_2 + AlH_3 and MgH_2 + Al (Molar ratio 1:1) and using DSC-MS (H_2) and XRD analysis. They found that when mixed with AlH_3, the dehydrogenation temperature of MgH_2 is reduced to 55 °C compared to MgH_2 alone, because of the interaction between MgH_2 and the oxide-free Al which was formed from desorption of AlH_3. Also, although AlH_3 is metastable and will not form after the first desorption reaction, MgH_2 + AlH_3 mixture showed improved hydrogen desorption/absorption kinetics compared to MgH_2 + Al.

Later, Liu et al. [11] investigated the hydrogen desorption properties of MgH_2/AlH_3 composites with molar ratios 1:1, 1:0.5, and 1:0.25. These authors found that the onset hydrogen desorption temperature of MgH_2 decreases when the amount of AlH_3 increases. The DSC and MS-H_2 results indicate that the mixtures MgH_2/AlH_3 exhibit a two-stage desorption process. The first one has been related to AlH_3 decomposition and the second one to the decomposition of MgH_2. Liu et al. [11] reported that the second stage is composed of two overlapping (peaks) desorption steps and showed that MgH_2 decomposes in two steps. In their work, XRD analysis of MgH_2 + 0.25 AlH_3 was performed on samples heated in the same conditions as the DSC-MS measurements at different temperatures. Liu et al. [11] concluded on the basis of DSC analysis and XRD results that desorption of Mg–Al–H alloys proceeds in two steps.

Andreasen [46] summarized the results of pressure–composition isotherms (PCIs) found in the literature and concluded that the de/hydrogenation of Al–Mg alloys is at least a two-step process when the β phase is present. Andreasen [46] also noted that, in most of the PCI studies on the Al–Mg alloys, the distinction of the plateau

pressures was difficult and uncertain because of the sloping of the measured curves and concluded that the thermodynamic parameters of the Al–Mg–H alloys calculated from these curves should be verified by more experiments. Tanniru et al. [5] characterized the hydrogenation behavior (in the temperature range of 180–280 °C) and PCIs (in the temperature range of 275–400 °C) of Mg-8 at% Al alloys compared to pure Mg to investigate the effect of Al addition on hydrogen storage properties of magnesium hydride. The PCI results showed that only one plateau was observed for Mg and Mg-8 at% Al alloys. However, the equilibrium pressure for hydride formation in Mg-8 at% Al alloys was slightly higher compared to pure Mg and the calculated enthalpy was lower by less than 10 %. The higher plateau pressures have been explained by the change of the thermodynamics of hydride formation due to the solubility of Al in hcp-Mg which, according to these authors [5], reduces the solubility of hydrogen in hcp-Mg. Also, sloped curves showing the rise of pressure with composition after the plateau region of the Al–Mg alloys have been observed by Tanniru et al. [5] and attributed to the hydrogenation of γ phase (to form MgH_2 and β). Later, Tanniru et al. [6] conducted PCI tests at 350 °C for Mg-10 at% Al and Mg-4 at% Al alloys. In the PCI experiments of Tanniru et al. [6], the pressure was increased in small steps and sufficient time was allowed for equilibrium to be reached in each step. For this reason, the results obtained by [6] will be compared with the calculations conducted in this work. Samples at different hydrogenation/dehydrogenation steps were analyzed using X-ray diffraction (XRD) and scanning electron microscopy (SEM) to study the microstructure evolution during PCIs. They [6] reported three steps for hydriding of Mg-10 at% Al alloys corresponding to three plateaus in PCIs at 350 °C. As for pure Mg, the PCI curve at 350 °C of Mg-4 at% Al alloys showed the existence of only the first plateau with a continuous increase of the pressure with the absorbed hydrogen. They [6] attributed the absence of the second and the third plateau for Mg-4 at% Al alloys to the small amount of γ phase formed at the end of the first plateau. In addition, Tanniru et al. [6] showed that the first plateau pressure increases with Al content of the samples and attributed this increase to kinetic factors. These results will be discussed and compared with the calculations done in this work in "Al–Mg–H system".

The Al–Mg–Na–H system

Investigations on hydrogen properties of mixtures of complex hydrides have been subject to many studies [7–9, 40, 47, 48]. Hudson et al. [40] was the first to report that, in the alanate mixture 0.5 $Mg(AlH_4)_2$ + $NaAlH_4$, the dehydriding temperature of $NaAlH_4$ was lowered by 50 °C and the desorption kinetics was four times faster. Sartori et al. [48] investigated the hydrogen storage properties of the composites $2MgH_2 + NaH + 3Al$ hydrided at 80 °C and 160 bar. They [48] described the decomposition reaction mechanism of the hydrided composite using TPD and XRD experiments. Ismail et al. [7–9] investigated the hydrogen storage properties and the reaction pathways of MgH_2–$NaAlH_4$ (4:1)/Na_3AlH_6 (4:1) composites using XRD, thermo-gravimetric analysis, DSC, TPD, and isothermal sorption measurements. Ismail et al. [7] showed that dehydriding kinetics of MgH_2 and $NaAlH_4$ were significantly improved when mixed together and reported that these hydrides destabilize mutually. Ismail et al. [9] reported that during the first step of the dehydrogenation reactions of the MgH_2–Na_3AlH_6 (4:1) composite where $NaMgH_3$, Al, and H_2 are formed, the decomposition of Na_3AlH_6 starts at a temperature 55 °C lower than the decomposition temperature of the as-milled Na_3AlH_6. In the second step, MgH_2 reacts with Al to decompose and to form the β (Al_3Mg_2) phase. The decomposition temperature of MgH_2 in the composite is also 55 °C lower than the decomposition temperature of the as-milled MgH_2 [9]. They [9] suggested that the observed thermodynamic and kinetic destabilization is a consequence of the in situ formation of β and $NaMgH_3$ phases during the dehydrogenation reactions of the MgH_2–Na_3AlH_6 (or $NaAlH_4$) (4:1) composites. In this work, the mechanisms of these reactions are discussed based on thermodynamic calculations.

Thermodynamic modeling

Pure elements

The Gibbs energy functions of the pure elements (Al, Mg, Na) and of pure liquids Al, Mg, and Na are taken from the compilation of Dinsdale [49]. The Gibbs energy of liquid monatomic hydrogen has been estimated by Ransley and Talbot [50] and is listed in Table 1.

Stoichiometric compounds

In the Al–Mg–Na–H system, the compounds $Al_{30}Mg_{23}$, AlH_3, MgH_2, $Mg(AlH_4)_2$, NaH, $NaMgH_3$, $NaAlH_4$, and Na_3AlH_6 are considered as stoichiometric compounds. Gibbs energy of a stoichiometric compound depends only on the Gibbs energy of the components and the Gibbs energy of formation, which is optimized using the experimental data (ΔH and ΔS of formation) from the literature.

Gas phase

The Gibbs energies of the gases included in this study, that is, Al, Al_2, AlH, H, H_2, Mg, Mg_2, MgH, Na, Na_2, and NaH,

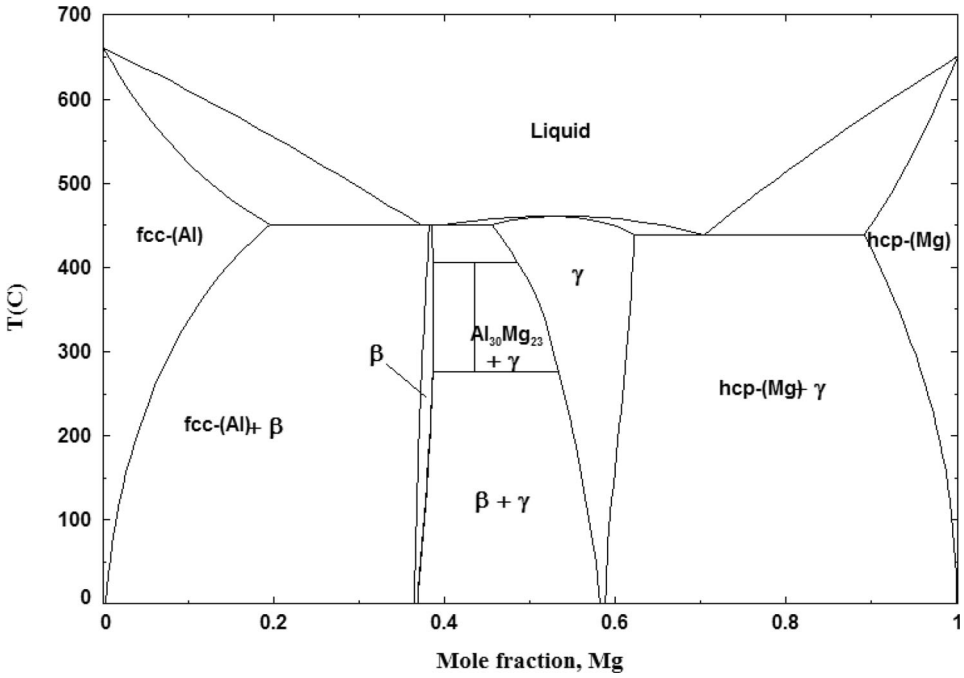

Fig. 1 Calculated Al–Mg phase diagram at 1 bar

are taken from FactPS database [12]. In the pressure range of interest, the non-ideal contribution of pressure to the Gibbs energy for the gases is very small. In fact, to account for the non-ideal contribution of hydrogen gas, Hemmes et al. [51] calculated the equation of state of hydrogen and other thermodynamic quantities in the range $p \leq 100$ GPa and $100 \leq T \leq 1000$ K. Numerical values of Gibbs energy and other quantities given in [51] have been used in this work to extrapolate the Gibbs free energy versus temperature of hydrogen gas at 100 bar and used in the calculations for comparison with the ideal gas model. A difference in temperatures of less than 3 K (at 100 bar) has been found. For this reason, all the gases are considered ideal gases.

Solid solution phase

Terminal solid solutions are modeled in this work using the compound energy formalism, as hydrogen atoms occupy the interstitial positions in the solid phases fcc-Al, hcp-Mg, and bcc-Na. These phases are described by two sublattices where Al, Mg, and Na are mixed randomly in the first sublattice to allow for their mutual solubility. Hydrogen atom and vacancy mix in the second sublattice. Therefore, as discussed in [2], $(Al, Mg, Na)_1(H, Va)_1$, $(Mg, Al, Na)_2(H, Va)_1$, and $(Na, Al, Mg)_1(H, Va)_3$ sublattices are used to model fcc-Al, hcp-Mg, and bcc-Na, respectively.

In the Al–Mg system, the compounds β (Al_3Mg_2) and γ ($Al_{12}Mg_{17}$) are taken from Harvey [14] where they are described by the sublattices $(Mg)_{10}(Al, Mg)_{24}(Al, Mg)_{24}$ and $(Al)_{19}(Al, Mg)_2(Mg)_{12}$ for γ and β, respectively.

Liquid phases

The modified quasichemical model (MQM) is used to model the liquid phase for all the binaries. Binary liquid parameters have been interpolated using the asymmetric Kohler–Toop technique where H is singled out as the asymmetric component as discussed in our previous paper [2]. No ternary parameters have been added to the liquid model.

Thermodynamic equations used to model different phases are explained in our previous paper [2].

Results and discussion

In "Thermodynamic description of the Al–Mg–Na–H system", the calculated thermodynamic properties and phase diagrams using the current database are presented for the binary and ternary phases discussed in "Thermodynamic description of Al–Mg–Na–H system". The thermodynamic parameters used in the present work for the Al–Mg–Na–H system are given in Table 1.

In "Hydrogen storage analysis of Al–Mg–Na–H system using thermodynamic modeling", thermodynamic calculations conducted to analyze and understand the hydrogen storage behavior of the Al–Mg–H and Al–Mg–Na–H systems are presented in comparison with the experimental

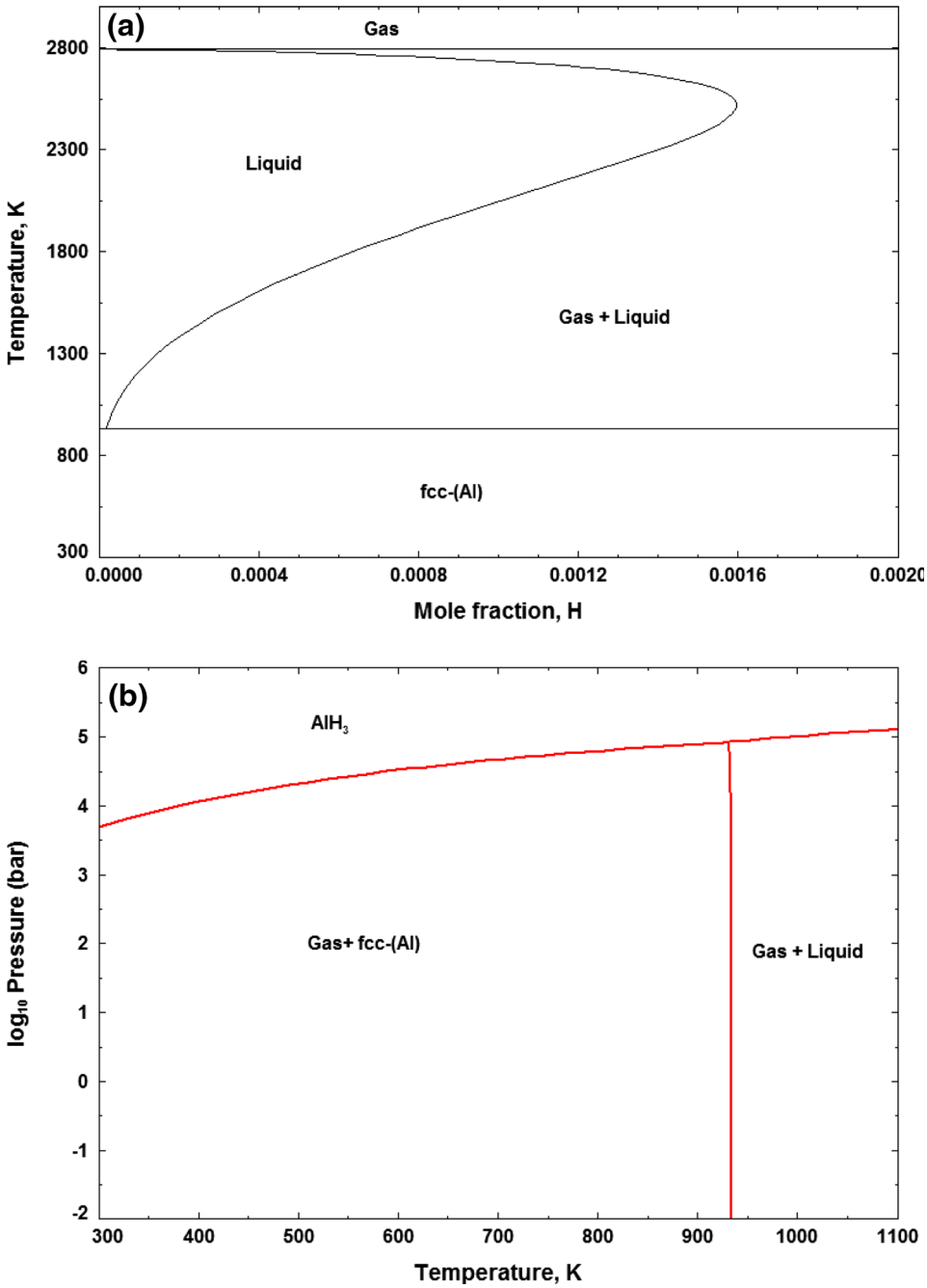

Fig. 2 Calculated Al–H phase diagram (**a**) and AlH3 pressure temperature diagram (**b**)

data cited in "Hydrogen storage behavior in Al–Mg–Na–H system".

Thermodynamic description of the Al–Mg–Na–H system

The Al–Mg and Al–H systems

The calculated Al–Mg and Al–H phase diagrams at 1 bar are presented in Figs. 1 and 2. Pressure temperature diagram for AlH_3 hydride is presented in Fig. 2b. It can be seen that AlH_3 is not stable under ambient temperature and pressure conditions.

The Al–Na system

The model parameters used in the Al–Na system are listed in Table 1. For the liquid phase, the parameters have been determined using the Na solubility in liquid Al [20–24] and Na activity in liquid Al [25, 26] experimental data. The

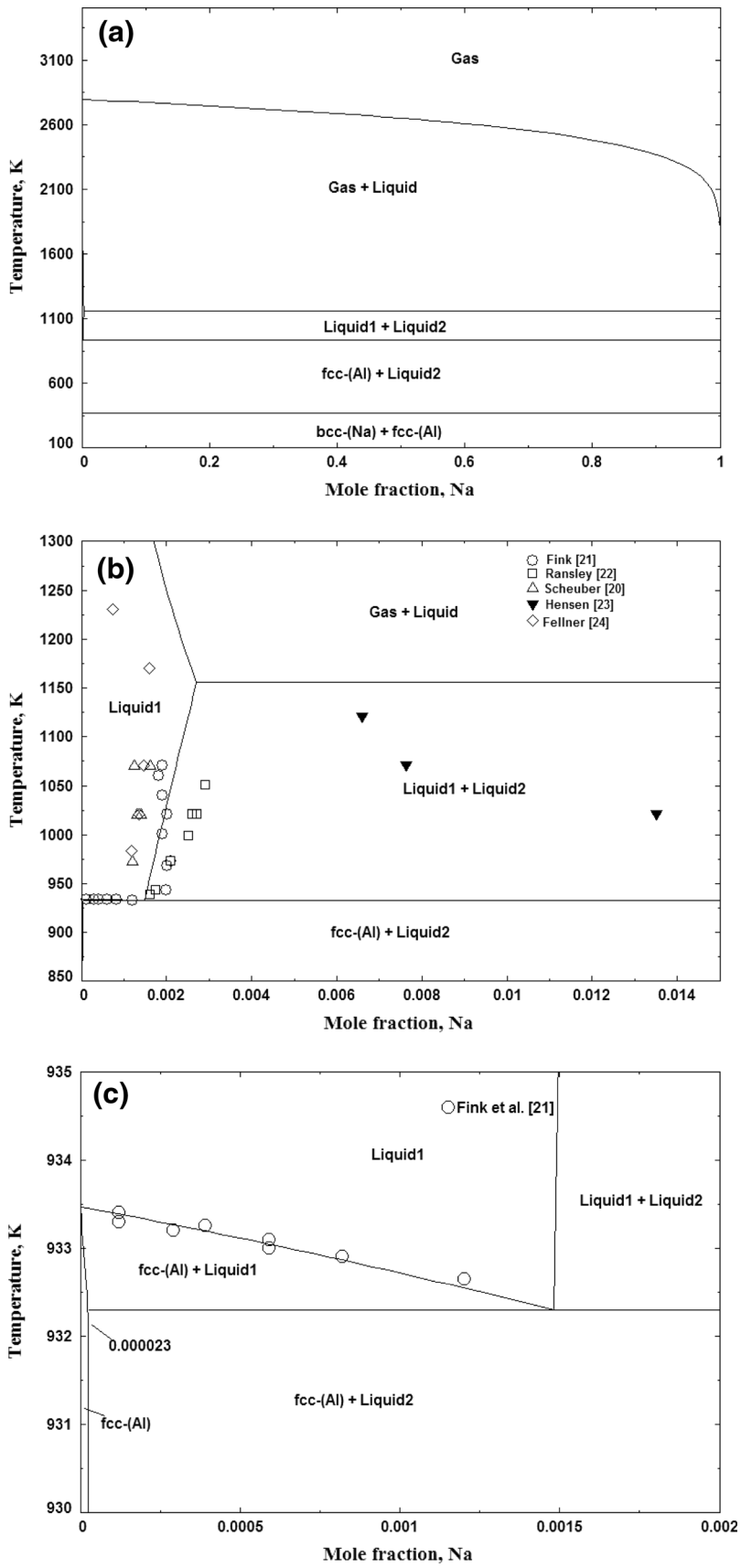

Fig. 3 **a** The calculated Al–Na phase diagram, **b** Al-rich side of Al–Na phase diagram in comparison with experimental data, **c** enlarged view of **b**

Table 2 Calculated invariant reactions in the Al–Na system in comparison with data from the literature

Reaction	Temperature (K)	Na concentration (at%)			References
Gas + liquid → Liquid 1 + Liquid 2	1155[c]	100	0.27	100	This work
	1157[c]	100	0.238	100	[19]
Liquid 1 + Liquid 2 → fcc-Al + Liquid 2	932[c]	0.15	0.0023	100	This work
	932[c]	0.14	0.002	100	[19]
	932[c]	0.18	0.0023	100	[18]
	932[ex]	0.18	<0.003	100	[21]
	932[ex]	0.14	0.002	100	[22]
fcc-Al + Liquid 2 → fcc-Al + bcc-Na	370.7[c]	100	0	100	This work
	371[c]	99.99	7.03×10^{-10}	100	[19]

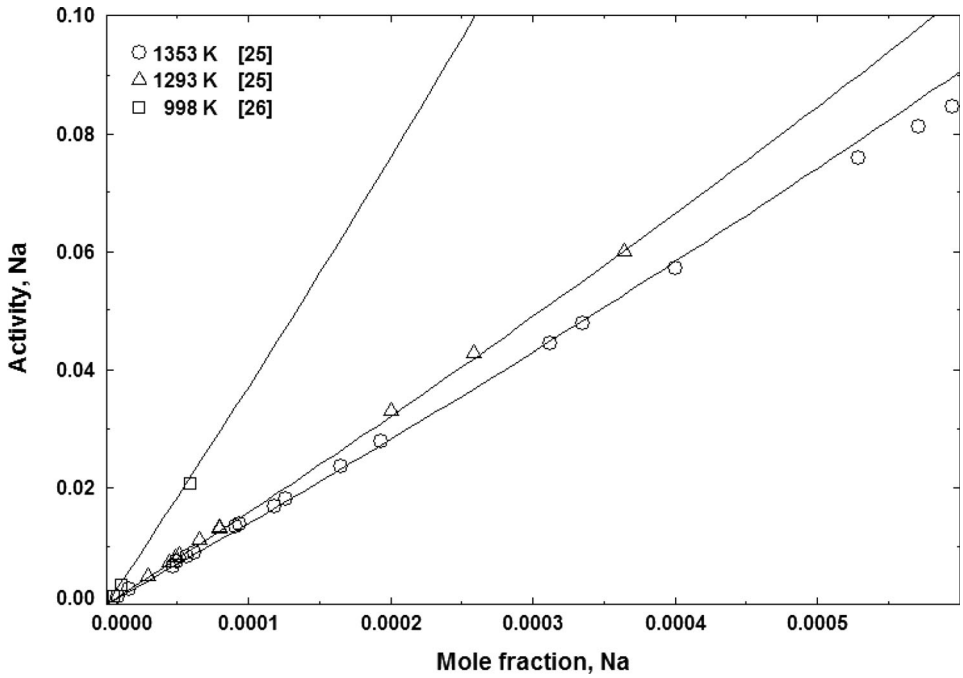

Fig. 4 The calculated activity of Na in liquid Al–Na in comparison with experimental data

calculated Al–Na phase diagram is presented in Fig. 3a. Figure 3b, c gives an enlarged view of the Al-rich part of the calculated phase diagram in comparison with experimental data. The experimental Na solubility in liquid Al results reported by Hensen et al. [23] are shown in Fig. 3b for comparison and have not been considered reliable in this work because of their disagreement with all the data reported in the literature. The calculated Na solubility in liquid Al shown in Fig. 3b are in reasonable agreement with the experimental data, especially those reported by Fink et al. [21]. In fact, as pointed out by Murray [18], the results of Scheuber et al. [20] are not certain due to hydrogen contamination. As can be seen in Fig. 3b, these results [20] are very close to those of Fellner et al. [24]. The experimental data reported by Ransley and Neufeld [22] have been given higher weight by Murray [18] and Zhang et al. [19] in their assessment of the Al–Na system because of high purity Al and the experimental procedure used. The calculated phase diagram by Murray fits the phase diagram data of Ransley and Neufeld [22]. However, Murray [18] did not consider recent Na solubility data and Na activity in liquid Al. The results presented in this work are in reasonable agreement with those of Zhang et al. [19]. The invariant reactions in the Al–Na system in comparison with experimental data and previous calculations are listed in Table 2.

The calculated activities of Na in Al–Na liquid at 1353, 1293, and 998 K in comparison with experimental data from the literature are presented in Fig. 4. There is a very good agreement between the calculated activity and the experimental data for Na concentrations below 0.04 at%. For Na concentrations above 0.04 at%, the calculated

Table 3 Thermodynamic properties of formation and decomposition of Mg(AlH4)2

RHeaction	Temperature, K	ΔH (kJ/mol)	References
$2Al + Mg + 4H_2 \rightarrow Mg(AlH_4)_2$	298.15	−79.1	This work
	298.15	−79.0[a]	[34]
	298.15	−80.33	[53]
	298.15	−82.8[a]	[35]
$Mg(AlH_4)_2 \rightarrow MgH_2 + 2Al + 3H_2$	298.15	1.8	This work
	435	1	[34]
	423	1.7	[36]
	435	0	[53]
	398–423	~0	[37]
	393	~2	[39]

[a] Calculated using the CALPHAD technique

activities at 1353 K are higher than the experimental data determined by Dewing [25]. As pointed out by Dewing [52], the experimental procedure (quenching) used in [25] may have been a source of errors.

The Al–Mg–H system

The calculated enthalpy of formation and decomposition of the $Mg(AlH_4)_2$ are given in Table 3 in comparison with data from the literature.

Good agreement is shown between the calculated heat of formation and decomposition of magnesium alanate and the calculations made by Palumbo et al. [34] and the experimental data of Claudy et al. [53].

The calculated temperature–pressure (PT) diagram for $Mg(AlH_4)_2$ is given in Fig. 5a. Figure 5b shows the calculated reaction path of $Mg(AlH_4)_2$ at 1 bar. Figure 5a shows that magnesium alanate is less stable than AlH_3 and will not form even at very high pressures. At 1 bar, $Mg(AlH_4)_2$ decomposes spontaneously to form MgH_2, fcc-Al, and gas phase. By increasing the temperature, MgH_2 decomposes to fcc-Al, β, and gas phase at 234 °C following reaction (2) as can be seen in Fig. 5b. These results are in good agreement with the literature. In fact, Palumbo et al. [34] calculated a temperature of 230 °C for reaction (2), and values in the range 217–240 °C have been reported using DSC experiments [36–38]. As mentioned in "Al–Mg–H system", Liu et al. [41] expressed fcc-Al as $Al_{0.9}Mg_{0.1}$ in Eq. (5) by taking into account the value of the maximum solubility of Mg in fcc-Al at 320 °C as 10 at%. However, that MgH_2 decomposition kinetics was poor during the experiments and MgH_2 started to release its hydrogen effectively at around 320 °C do not indicate clearly that the composition of fcc-Al corresponds to its equilibrium composition at 320 °C.

In Fig. 5b, the different phases are presented with different colors and the Al and Mg components of each phase are presented with dotted and dashed lines, respectively, with the same color as the phase. Figure 5b shows that the decomposition of MgH_2 is preceded by a gradual decrease in the amount of MgH_2, caused by its partial gradual decomposition with an increase in the amount of fcc-Al in which the produced Mg has dissolved.

According to these calculations, the composition of fcc-Al at 234 °C is 94.89 % Al, 5.10 % Mg, and 2.5×10^{-7} % H, which shows that the solubility of hydrogen in fcc-Al is negligible at this temperature and the solubility of Mg in fcc-Al is equal to its solubility limit in the Al–Mg system at this temperature (Fig. 1).

The calculated vertical section of the Al–Mg–H_2 phase diagram at 100 and 230 °C is presented in Fig. 6. It shows that the composition of the hydrided Al–Mg system depends on the hydrogen gas amount added. Above 0.5 mol fraction H_2, the system is composed of gas, fcc-Al, and MgH_2 phases in proportions depending on the relative amounts of Mg and Al.

The Al–Mg–Na system

There are no experimental data for the Al–Mg–Na ternary system; the calculated isothermal sections at 100 and 500 °C are presented in Fig. 7. Liquid 2 corresponds to liquid Na and Liquid 1 to liquid Al–Mg. Figure 8 shows the calculated vertical section of the Al–Mg–Na system along the composition line AlNa–Mg at 1 bar in comparison with the Al–Mg phase diagram (dotted red line). The presented vertical sections reproduce the phase relations and the miscibility gaps in the binary phase diagrams. It can be seen that Na does not affect the phase relations in the Al–Mg phase diagram at 1 bar except the presence of bcc-Na or liquid Na, which shows the limited solubility of Na in hcp-Mg, fcc-Al, and the Al–Mg compounds. Only a small decrease in the melting point of hcp-Mg is observed when Na is added to the Al–Mg mixture.

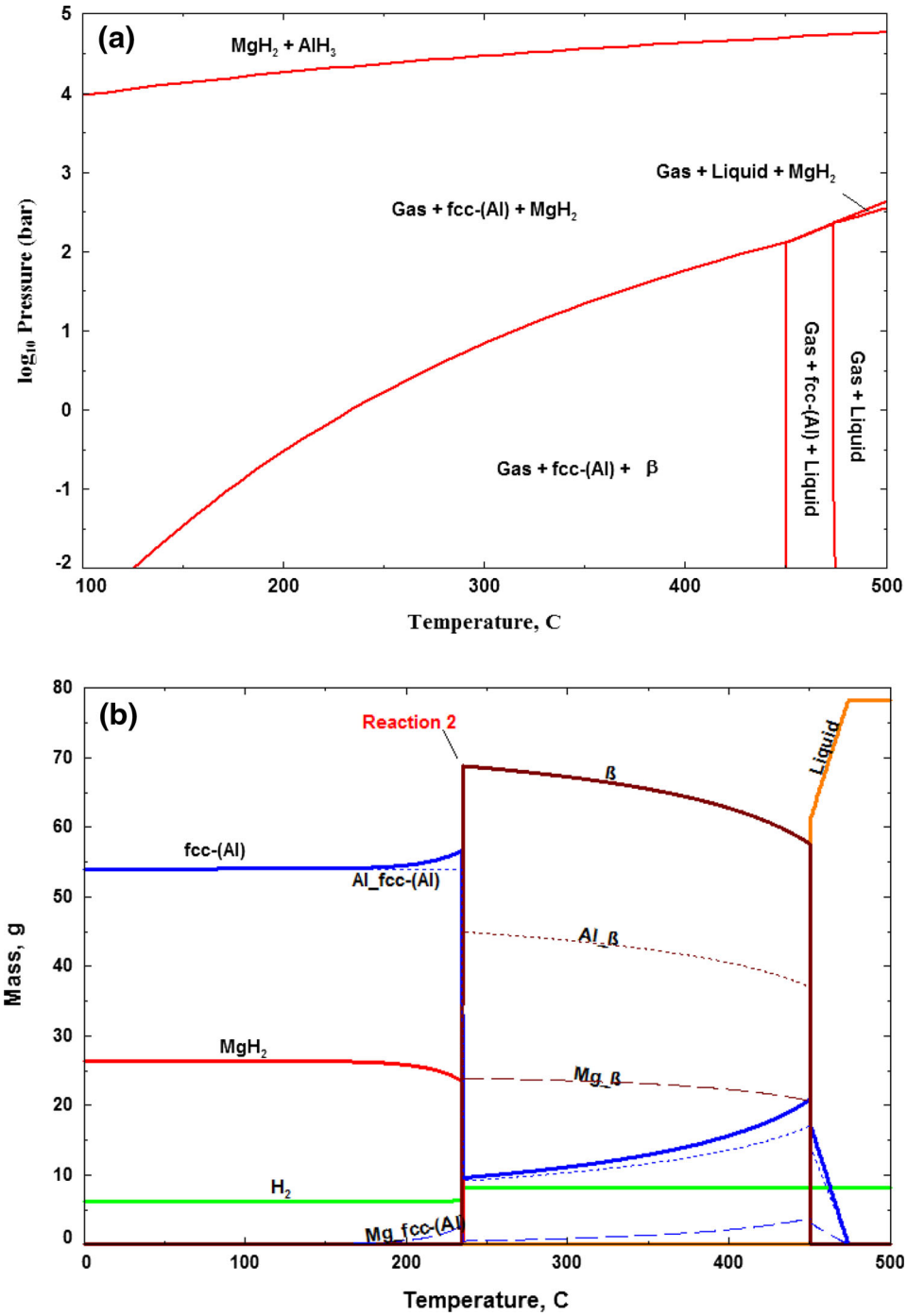

Fig. 5 **a** P–T diagram and **b** decomposition reaction path of $Mg(AlH_4)_2$ at 1 bar

The Al–Na–H system

The calculated PT diagrams of $NaAlH_4$ is presented in Fig. 9. It shows the evolution of the decomposition temperature of sodium alanates with pressure. $NaAlH_4$ decomposes in two steps following Eqs. 3 and 4 and the decompositions temperatures at 1 bar are 21.45 and 106.58 °C, respectively. At 10 bar, these temperatures increase to 81.68 and 179.02 °C for reactions 3 and 4, respectively.

The calculated isothermal sections of the Al–Na–H_2 system at room temperature, at 1 and 10 bar, are presented in Fig. 10 to show the phase relations in these conditions.

To show the stability of the hydrides and their decomposition temperatures in this system, vertical sections at different pressures can be calculated using the database

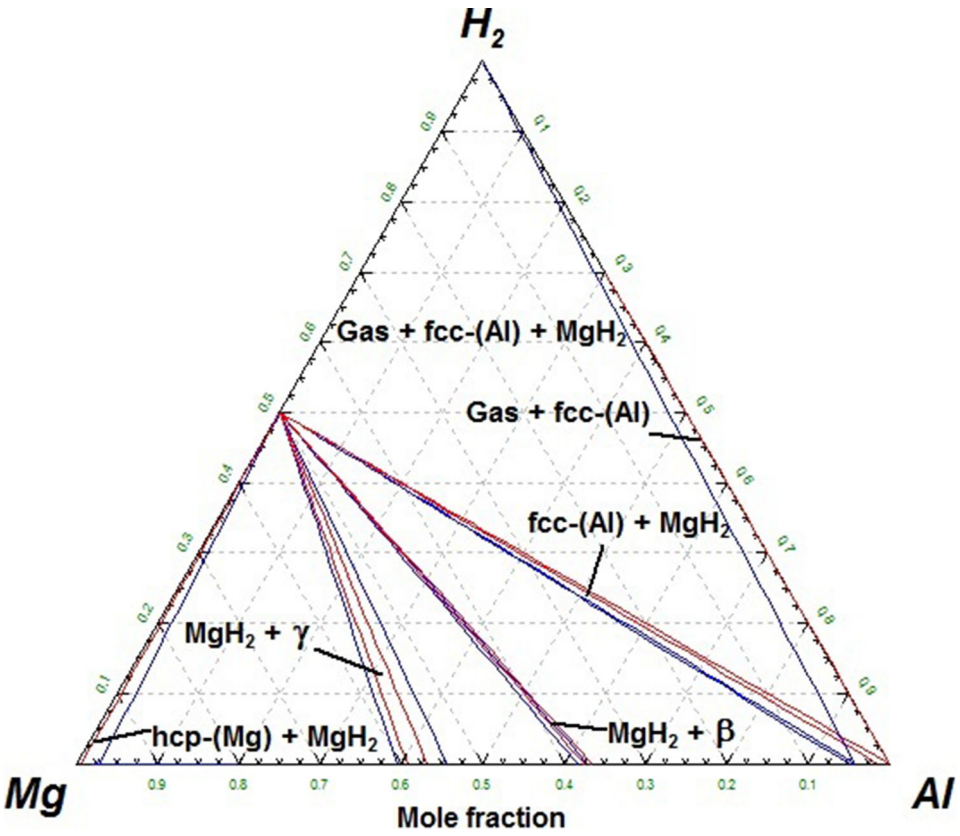

Fig. 6 The calculated isothermal section of the Al–Mg–H_2 phase diagram at 100 °C (in *red*) and 230 °C (in *blue*)

developed in this work. As an example, the calculated vertical sections along the composition line AlH_3–NaH at 1 and 10 bar are shown in Fig. 11.

Hydrogen storage analysis of the Al–Mg–Na–H system using thermodynamic modeling

The Al–Mg–H system

The calculated phase diagram of $MgH_2 + AlH_3$ at 1 bar is presented in Fig. 12a. An enlarged view of the MgH_2-rich part of MgH_2–AlH_3 phase diagram is presented in Fig. 12b. It can be seen that the MgH_2 decomposition process depends on Al content. Five regions are identified in Fig. 12a separated by blue dotted lines. For the AlH_3 mole fraction below 0.045, the decomposition of MgH_2 occurs in four steps according to the following reactions (the third and the fourth steps can be seen in Fig. 12b):

The decomposition temperature of the last reaction in Eq. (7) varies from 284.73 °C for pure MgH_2 to 283.3 °C for 0.045 mol fraction of Al as can be seen in Fig. 12b. This small difference can be explained by the solubility of Al in hcp-Mg.

For AlH_3 between 0.045 and 0.46 mol fraction, MgH_2 decomposes in three steps. For AlH_3 between 0.46 and 0.63 mol fraction, decomposition proceeds in two steps. For AlH3 content between 0.63 and 0.95 mol fraction, MgH_2 decomposes in only one step at 234 °C. It should be noted that, for AlH_3 content starting from the 0.95 mol fraction, the decomposition temperature of MgH_2 decreases with increasing Al content.

The predicted reactions in the system are compared with the results of Liu et al. [10] on the dehydrogenation process of the $MgH_2 + AlH_3$ mixture. This composition corresponds to 0.5 mol fraction of AlH_3 in Fig. 12a where it is marked by a red dotted line.

$$\mathrm{MgH_2 + fcc\text{-}Al \xrightarrow{234^\circ C} MgH_2 + \beta + H_2 \xrightarrow{257.8^\circ C} MgH_2 + \gamma + H_2 \xrightarrow{283.3^\circ C} MgH_2 + hcp\text{-}Mg + H_2 \xrightarrow{284.7< T^\circ C< 283.3} hcp\text{-}Mg + H_2} \quad (7)$$

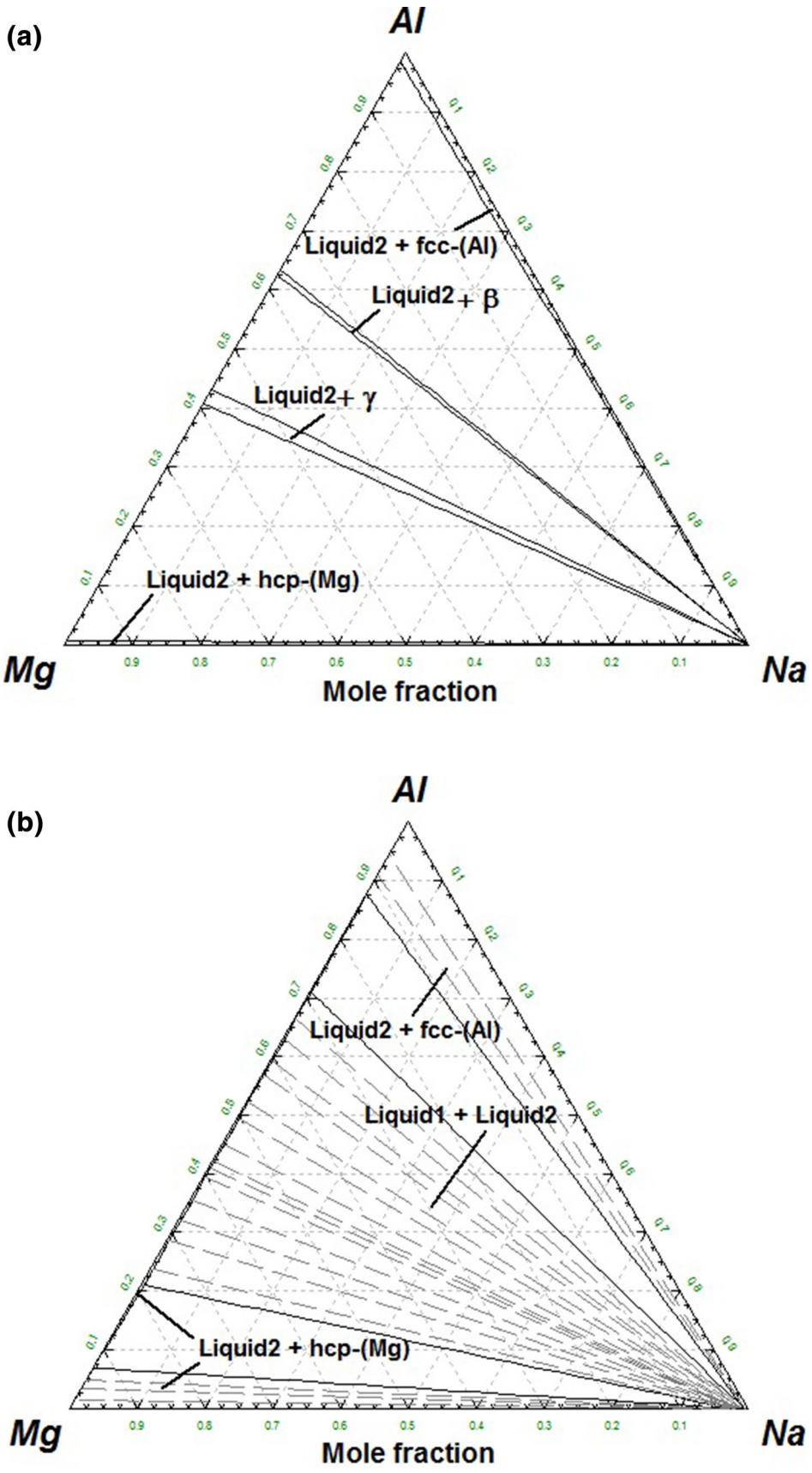

Fig. 7 The calculated Al–Mg–Na isothermal sections at 1 bar and **a** 100 °C and **b** 500 °C

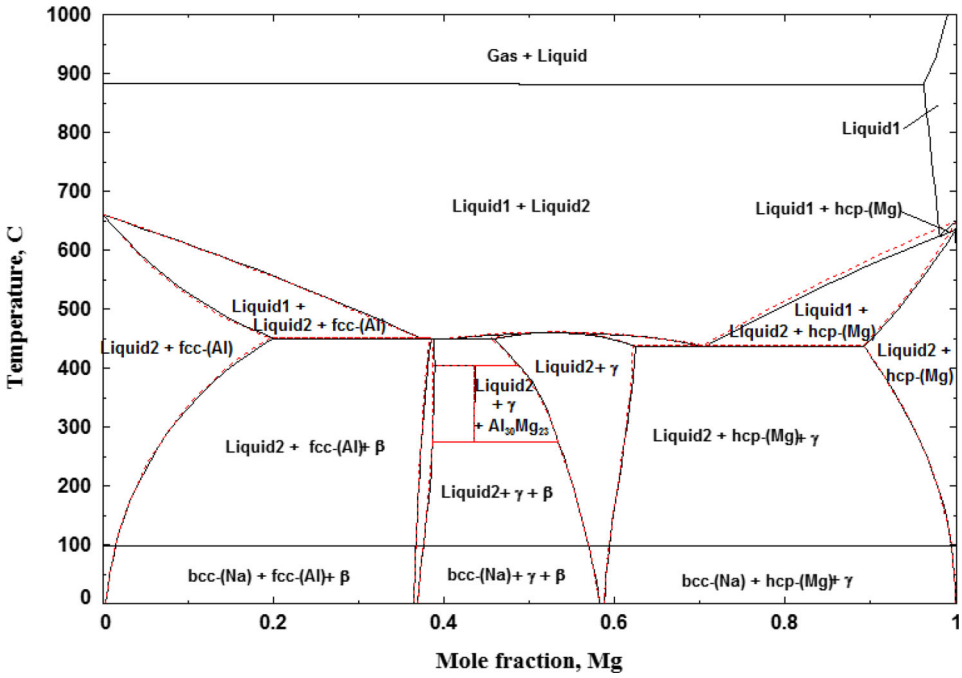

Fig. 8 Calculated vertical section of the Al–Mg–Na system along the composition line AlNa–Mg compared to the calculated Al–Mg phase diagram (*dashed line*) at 1 bar

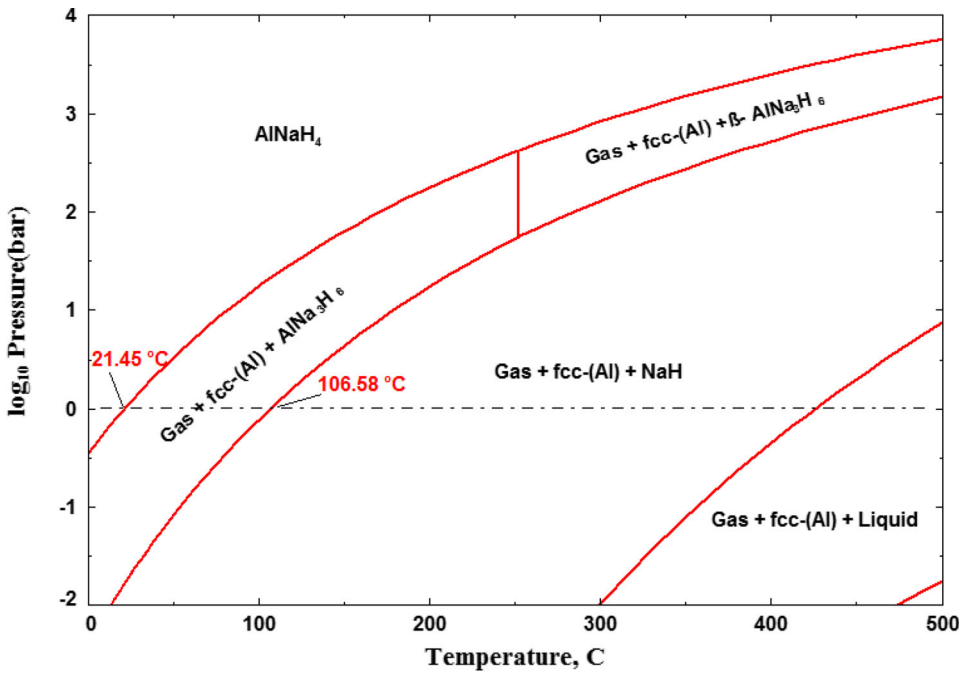

Fig. 9 P–T diagram of $NaAlH_4$

First, Liu et al. [10] reported that the decomposition temperature of MgH_2 in the mixture is reduced by 55 °C compared to the pure MgH_2 and attributed this decrease to the interaction between MgH_2 and Al. According to our previous paper [2], the theoretical decomposition temperature of MgH_2 is 284.73, 50.73 °C higher than the calculated first decomposition step in this mixture (234 °C), which is consistent with the results of Liu et al. [10]. However, the temperatures they [10] reported were higher as a result of the slow kinetics and the long time required to reach equilibrium [10]. Temperatures in the ranges 217–250 °C (DSC) [36, 37] and 210–220 °C (in situ XRD) [36] have also been reported.

In their second investigation on the thermal decomposition of MgH_2/AlH_3 composites, Liu et al. [11], using DSC and MS-(H_2), found that the onset and peak temperatures of the first decomposition of MgH_2 in the mixtures decrease with increase in the amount of AlH_3. The onset

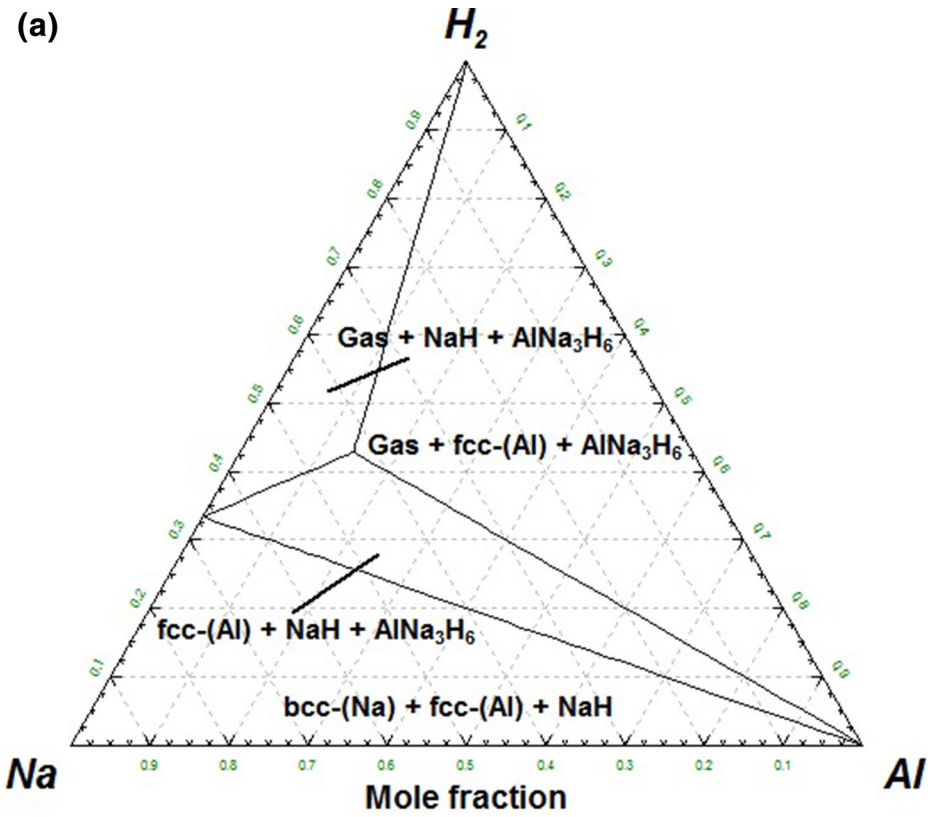

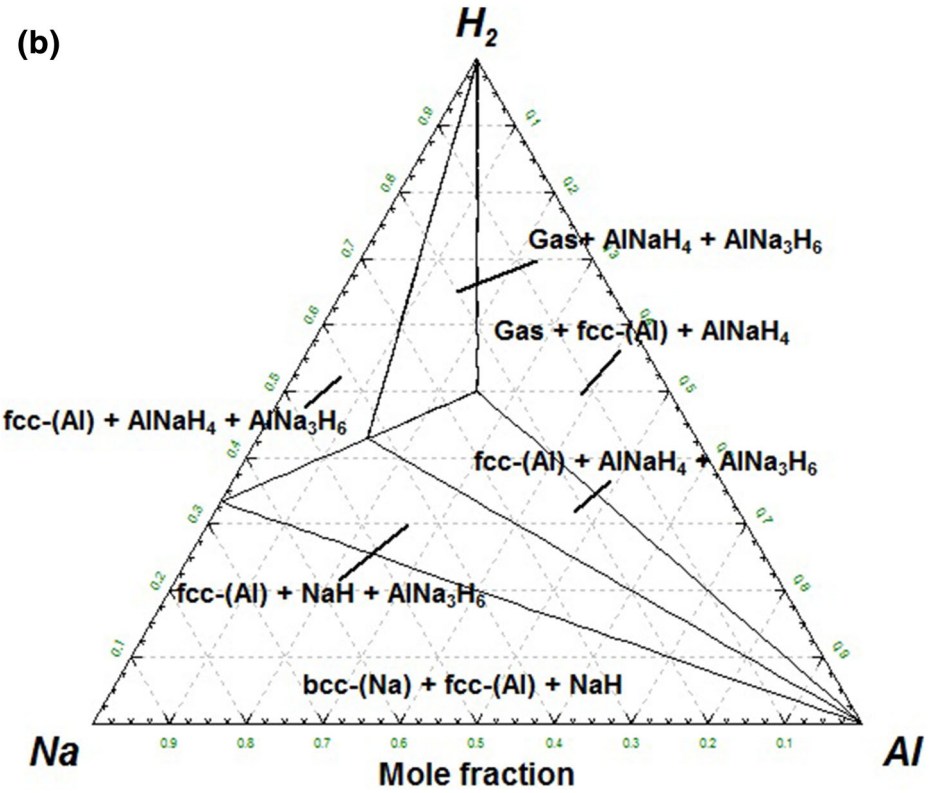

Fig. 10 The calculated Al–Na–H_2 isothermal section at 25 °C and **a** 1 bar and **b** 10 bar

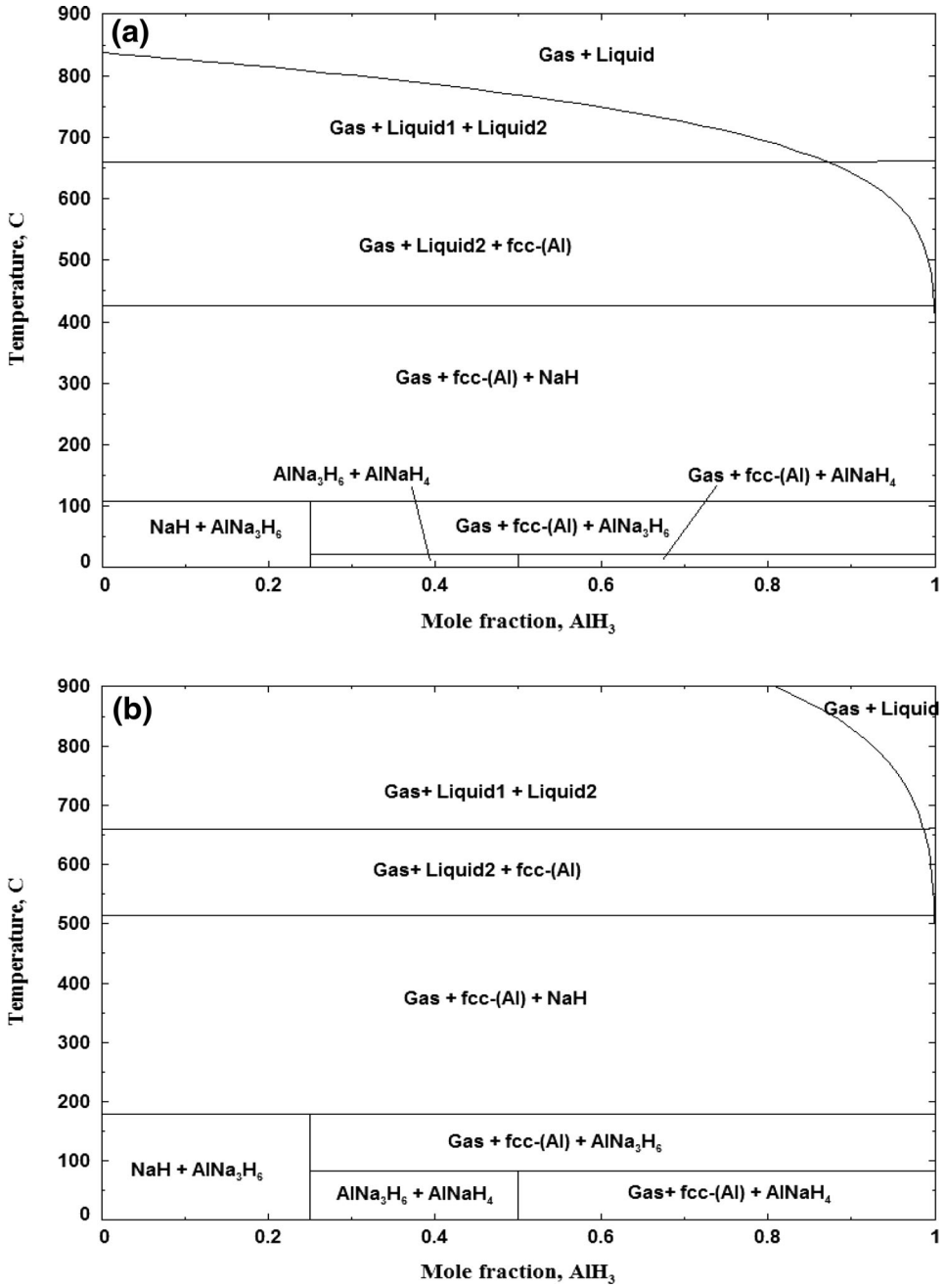

Fig. 11 The calculated AlH_3–NaH vertical section at **a** 1 bar and **b** 10 bar

temperatures were 252, 248, and 243 °C for MgH_2/AlH_3 composites with molar ratios 1:0.25, 1:0.5, and 1:1, respectively. The reported onset temperature for the first decomposition of MgH_2 [11] approaches gradually the calculated value of 234 °C. This indicates that AlH_3, in addition to destabilizing MgH_2, improves its decomposition kinetics.

Second, Liu et al. [10] reported three stages during the thermal decomposition of the mixture $MgH_2 + AlH_3$ using DSC-MS (H_2). The first stage was related to the decomposition of AlH_3. The second stage, which might be composed of two overlapping peaks [10], was attributed to the reaction of MgH_2 and Al to form the γ phase. The last step was attributed to the melting of the γ phase. AlH_3, as shown in Fig. 2b, is not stable in normal conditions and will decompose spontaneously. The first stage observed by Liu et al. [10] can be explained by poor kinetics.

In Fig. 12a, the thermal decomposition steps of $MgH_2 + AlH_3$ composite can be followed along the dotted red line, marking this composition. The process is as follows:

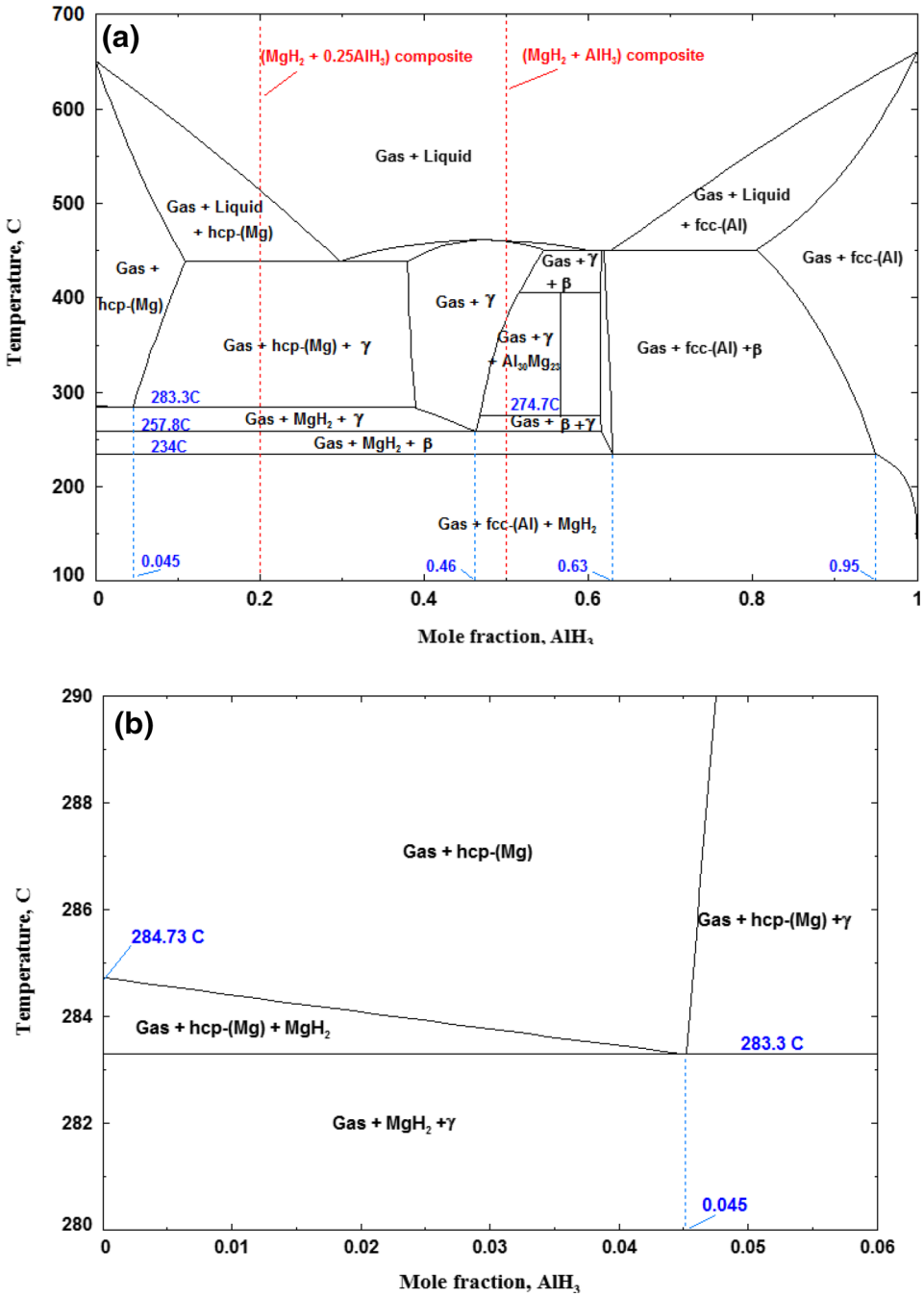

Fig. 12 **a** The calculated MgH_2–AlH_3 phase diagram at 1 bar; **b** an enlarged view of **a**

$$MgH_2 + \text{fcc-Al} \xrightarrow{234^\circ C} MgH_2 + \beta + H_2 \xrightarrow{257.86^\circ C} \beta + \gamma + H_2 \xrightarrow{274.76^\circ C} Al_{30}Mg_{23} + \gamma + H_2 \xrightarrow{379.4^\circ C} \gamma + H_2 \xrightarrow{458.98<T^\circ C<460.16} \text{Liquid} + H_2 \quad (8)$$

Equation (8) shows an overall agreement with the results of Liu et al. [10] and gives a more detailed description of the process. This can be explained by the fact that the process suffers from poor kinetics and that the reaction temperatures are too close to observe distinct steps using DSC-MS (H_2) experiments. However, XRD analysis

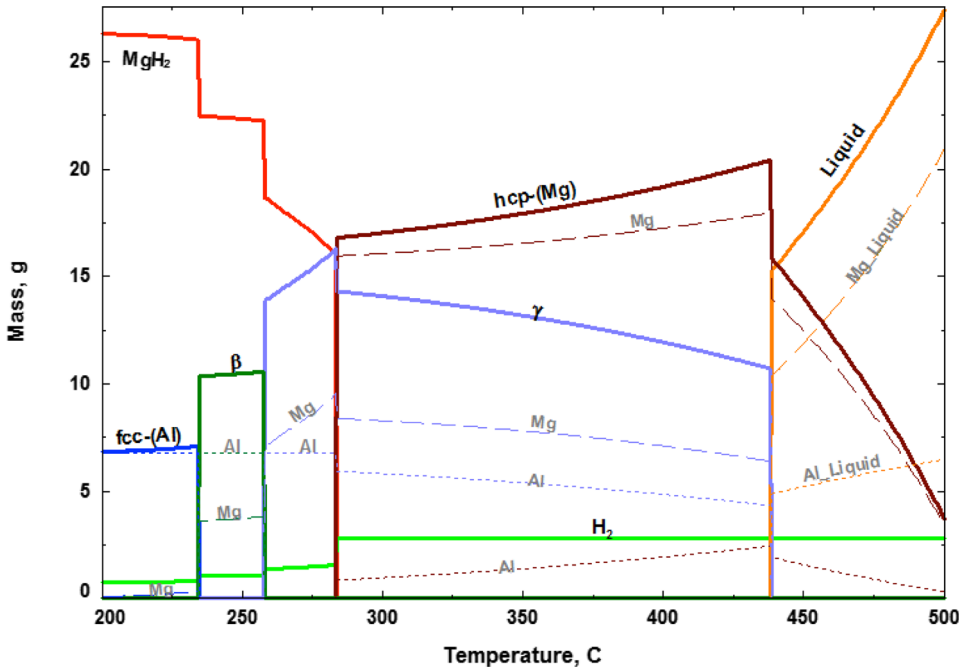

Fig. 13 Reaction path of $MgH_2 + 0.25AlH_3$ showing the phase assemblage with temperature

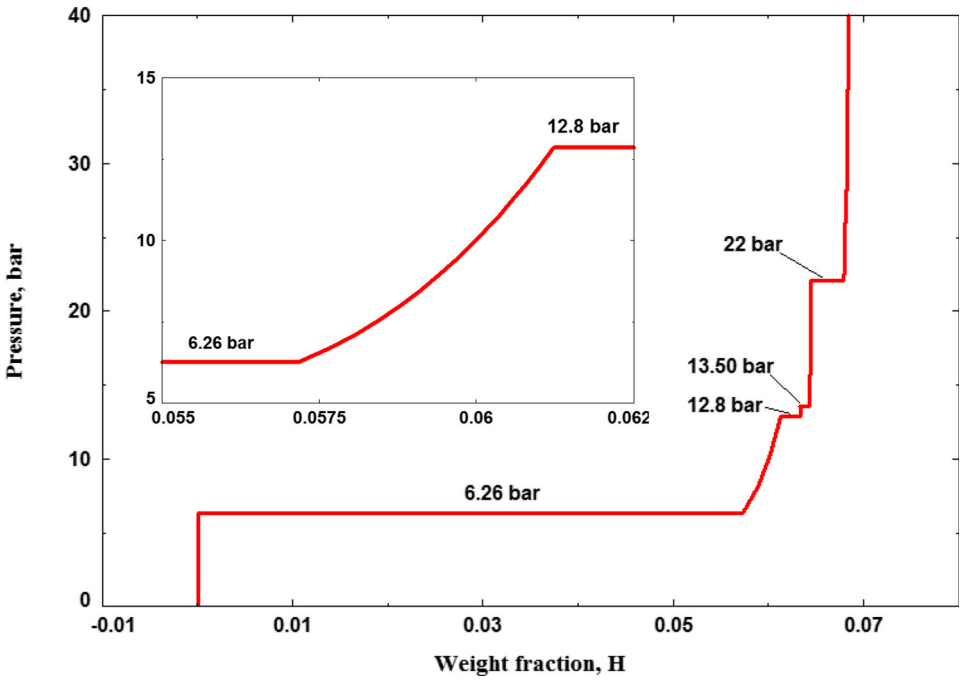

Fig. 14 Calculated PCI curve of Mg-10 at% Al at 350 °C

[10] showed that the mixture was composed of MgH_2 and Al at 200 °C, and of γ phase at 400 °C, which is consistent with the calculations shown in Eq. (8) and Fig. 12a.

Liu et al. [11] investigated the structure evolution during desorption of $MgH_2 + 0.25AlH_3$ composites using XRD analysis of samples heated to various temperatures (from 175 to 400 °C) with the same heating rate as in DSC-MS (H_2) experiments. They [11] reported a shift in the diffraction peaks of Al to small angles and the formation of β phase when the temperature was increased from 250 to 310 °C. They [11] attributed the Al peak shift to Mg atom dissolution in Al lattice causing its expansion until saturation where the new phase, β (Al_3Mg_2), formed. However, Liu et al. [11] neglected the fact that this peak shift might also be caused by thermal expansion of the Al lattice.

In the following step, MgH_2 reacts with β to form the γ phase [11]. In the final step, the residual MgH_2 decomposes and only Mg solid solution and γ phase were detected [11].

In Fig. 12a, the thermal decomposition steps of $MgH_2 + 0.25\ AlH_3$ composite can be followed along the dotted red line marking this composition. It shows a very good agreement with the results of Liu et al. [11] concerning the structure evolution of the composite. From Fig. 12a, the decomposition process of MgH_2 in the composite is as follows:

$$MgH_2 + \text{fcc-Al} \xrightarrow{234^\circ C} MgH_2 + \beta + H_2 \xrightarrow{257.86^\circ C} MgH_2 + \gamma + H_2 \xrightarrow{283.23^\circ C} \text{hcp-(Mg)} + \gamma + H_2 \quad (9)$$

Equilibrium calculations of the reaction path provide more information about the amount of phases and their composition during the thermal decomposition of the composite. In Fig. 13, the calculated reaction path of $MgH_2 + 0.25AlH_3$ composite at 1 bar is shown. The amount of phases is expressed in grams and is presented in solid lines with different colors for each phase. The amount of Al and Mg in each phase is presented with the same color as the phase, with dotted and dashed lines for Al and Mg, respectively. It can be seen that, for temperatures above 200 °C, the amount of fcc-Al (blue solid line) increases smoothly wth temperature, while the amount of MgH_2 (red solid line) decreases. Simultaneously, the Al content of fcc-Al (blue dotted line) is constant and the Mg content of fcc-Al (blue dashed line) increases smoothly, which proves that Al destabilizes MgH_2 at these temperatures and the resulting Mg atoms dissolve in fcc-Al and increase its amount until the temperature of 234 °C, where the solubility limit of Mg in fcc-Al is reached and β forms. This conclusion agrees very well with the XRD results reported in the literature [11, 38, 39, 41], observing the Al peak shift in the MgH_2/Al composites with increasing temperature until it disappears and the β formation occurs.

In Fig. 13, at 234 °C, it is seen that the formation of β (presented with a dark green solid line) is accompanied by an abrupt decrease in the amount of MgH_2 (the solid red line). A close look at Al and Mg content in β shows that the amount of Mg in β (dashed green line) increases abruptly at 234 °C. This can be explained by the more important solubility of Mg in β. Since the first effective decomposition step of MgH_2 in MgH_2–Al mixtures is at 234 °C, It can be concluded that the first effective destabilization step of MgH_2 by Al is due to the formation of β. The same conclusions can be formed regarding the second step decomposition of MgH_2 at 257.86 °C accompanied by the formation of γ. For temperatures between 257.86 and 283.23 °C, the amount of MgH_2 decreases with temperature, while the amount of γ increases simultaneously with the increase of the amount of Mg dissolved in it (purple dashed line). It should be noted that the amount of Al dissolved in the β and γ phases (dotted green and purple lines) is constant. At 283.23 °C, the residual MgH_2 decomposes resulting in the hcp-Mg phase.

The calculated PCI curve at 350 °C for Mg-10 at% Al alloy is presented in Fig. 14 and shows the presence of four plateau regions at 6.26, 12.8, 13.5, and 22 bar. The calculated hydriding reaction path of Mg-10 at % Al alloy at 350 °C is presented in Fig. 15. According to Figs. 13 and 14, the initial composite is composed of hcp-Mg and γ phases. The first plateau corresponds to the formation of MgH_2 and an additional γ phase from hcp-Mg. The second plateau corresponds to the hydriding of the γ phase to produce MgH_2 and $Al_{30}Mg_{23}$. The third plateau is attributed to the hydriding of $Al_{30}Mg_{23}$ to produce MgH_2 and β. The forth plateau corresponds to the hydriding of the β phase to produce MgH_2 and fcc-Al.

The results shown in Figs. 14 and 15 are compared to the experimental data reported by Tanniru et al. [6]. These authors [6] reported the PCI curve at 350 °C and the microstructural evolution of the samples (Mg-10 at% Al) during the measurements. However, they [6] could not identify the plateau pressures directly from the PCI curve because of the sloped and not well-defined plateaus resulting from the poor kinetics in addition to the small amount of hydrogen absorbed (below the theoretical capacity of the sample). For these reasons, a direct comparison between the calculated and the measured PCIs [6] is not possible. Nevertheless, the calculated plateau pressures are compared to those identified by Tanniru et al. [6]. Three hydriding steps corresponding to three plateaus at 6.2, 12.7, and 22 bar have been reported [6]. These results [6] are in very good agreement with the current calculations shown in Fig. 14 except for the calculated plateau pressure at 13.5 bar, which was not observed by these authors. This can be attributed to the small difference of pressure with the preceding step (12.8 bar) and the small length of the plateau in addition to the poor quality of the curve. Also, microstructural analysis and phase identification at different stages of hydriding/dehydriding

experiments reported by Tanniru et al. [6] are in good agreement with this work. However, these authors [6] did not report the formation step of $Al_{30}Mg_{23}$ and therefore they combined the two-step hydriding reaction: (γ to $Al_{30}Mg_{23} + MgH_2$ at 12.8 bar and $Al_{30}Mg_{23}$ to $\beta + MgH_2$ at 13.5 bar) in only one step: (γ to $\beta + MgH_2$ at 12.7 bar). In Fig. 15, the amounts of Al and Mg in each phase are presented by dotted and dashed lines, respectively, with the same color as the phase. It can be seen in Fig. 15 that from a pressure of 6.26 and 12.8 bar, the alloy is composed of γ phase and MgH_2 and the amount of MgH_2 increases gradually in this pressure range, while the amount

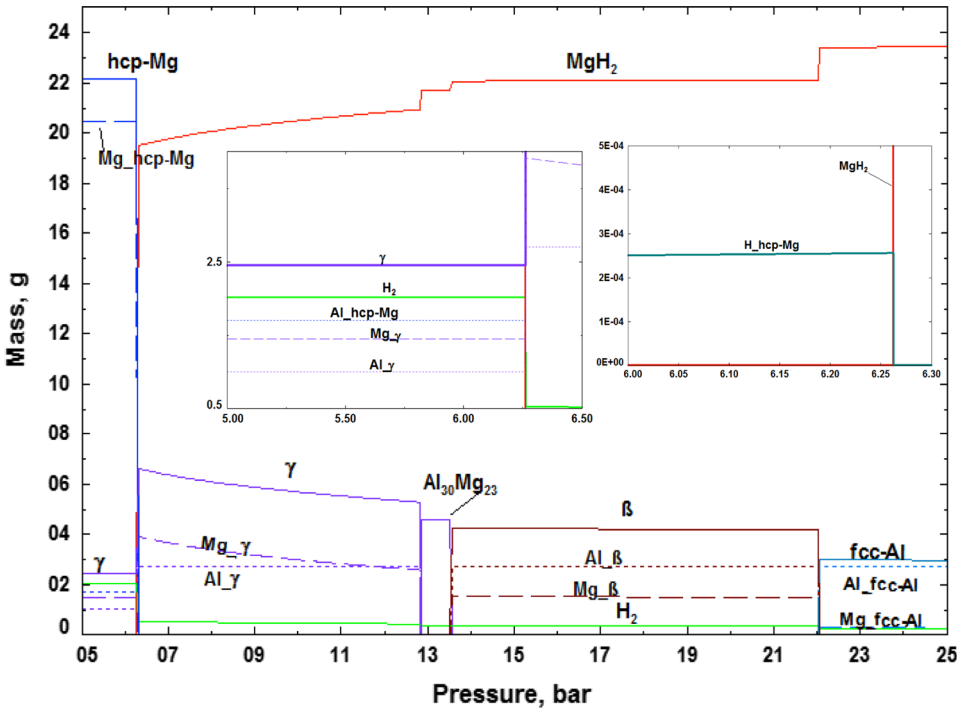

Fig. 15 Hydriding reaction path of Mg-10 at% Al at 350 °C

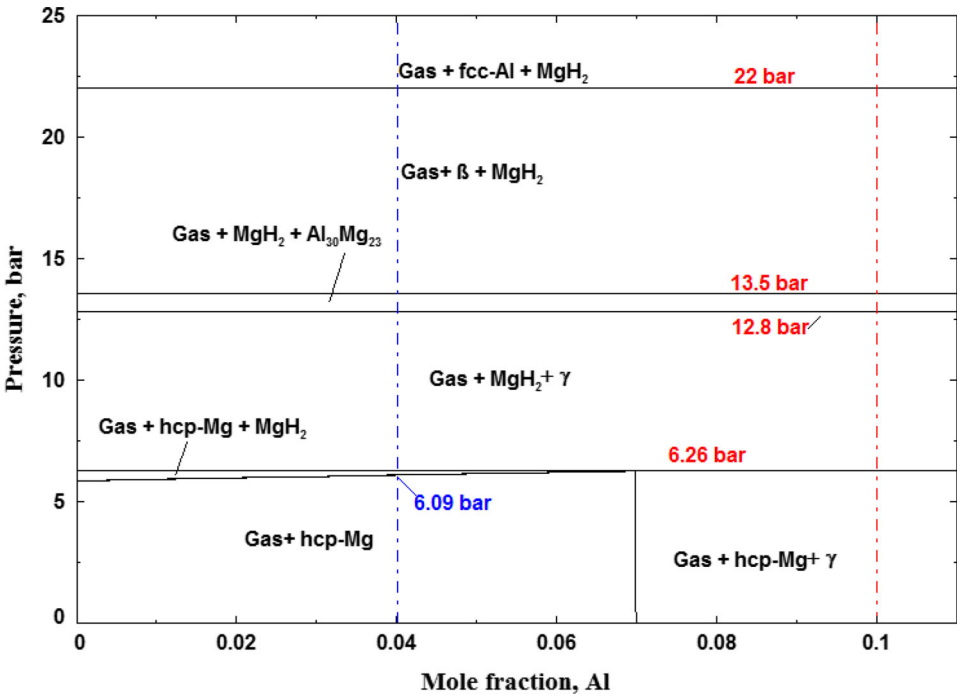

Fig. 16 The calculated MgH_2–Al phase diagram at 350 °C

of Mg in the γ phase decreases and the amount of Al in the γ phase is constant, which signifies that the γ phase is more concentrated in Al. This step takes the form of a curved line in PCI curves (the enlarged inset in Fig. 14) and is due to the large solubility range of the γ phase. Bouaricha et al. [54] reported that the PCI curves of Mg–Al alloys with γ phase compositions showed sloped plateau between 8 and 15 bar, which is consistent with the trend of the PCIs calculated in this work. It can be concluded that the PCI inclined plateaus reported in the literature [46] for the Al–Mg alloys, is, in addition to kinetic factors, due to the large solubility range of the γ phase, short plateaus' length, and the small differences between the last three plateau pressures.

Tanniru et al. [6] reported that the first plateau pressures increased on increasing Al content (5.4, 5.7, and 6.2 bar for Mg, Mg-4 at% Al, and Mg-10 at% Al, respectively) and attributed this raise in pressure to kinetic factors. To investigate the variation of the first plateau pressure with Al content, the calculated phase diagram of MgH_2–Al [Al content between 0 and 11 at% (0.11 mol fraction)] alloy at 350 °C is presented in Fig. 16.

It shows that for Al content above 7 at%, the starting alloy is composed of hcp-Mg and γ phase and the hydriding of these alloys follows the same processes as for the Mg-10 at% Al alloys presented in Figs. 13 and 14. Mg-10 at% Al composition is marked with dashed red line in Fig. 16, which shows the four-hydriding steps with increase in the pressure. For Al content below 7 at%, the starting alloy is composed of hcp-Mg, and an additional step in the hydriding of alloys with these compositions is shown. This step occurs at a pressure which depends on the Al content and ranges between 5.84 bar for pure Mg to 6.26 bar for Al content of 7 at%. As example, Mg-4 at% Al composition is marked with dashed blue line in Fig. 16 and shows that the first hydriding step for alloys with this composition occurs at 6.09 bar. The calculated PCI curve at 350 °C for Mg-4 at% Al alloy is presented in Fig. 17. The enlarged portion of the first plateau shows that what can be seen as one plateau pressure is in fact composed of a curved portion starting at 6.09 bar followed by a straight one at 6.26 bar. Of course, this difference could not be observed in the experimental PCI [6], but it explains the variations in the first plateau pressure with Al content reported by Tanniru et al. [6].

Figure 18 shows the calculated hydriding reaction pathway of Mg-4 at% Al alloy at 350 °C for pressures near the first plateau pressure. It shows that MgH_2 starts forming at a pressure of 6.09 bar and its amount (red line) increases gradually with decreasing amount of hcp-Mg (blue line) as the pressure increases. The amount of Al dissolved in hcp-Mg (blue dotted line) is constant, while the amount of Mg in hcp-Mg (blue dashed line) decreases, which means that the hcp-Mg phase is more concentrated in Al while MgH2 is forming. The enlarged view shows that the amount of H in hcp-Mg decreases with the pressure too. At 6.26 bar, hcp-Mg is hydrided and the γ phase forms. It can be concluded from the calculations shown in Figs. 15, 16, and 17

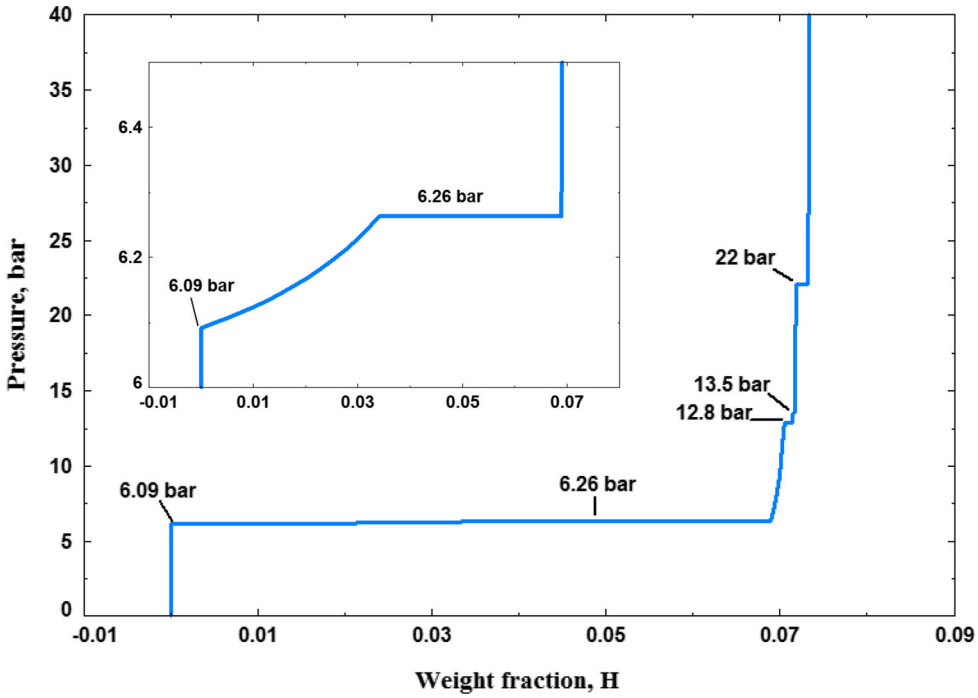

Fig. 17 Calculated PCI curve of Mg-4 at% Al at 350 °C

that the variations in the first plateau pressure reported in the literature is due to the solubility of Al in hcp-Mg and not to kinetic factors as suggested by Tanniru et al. [6].

The Al–Mg–Na–H system

As mentioned in "Al–Mg–Na–H system", Ismail et al. [7–9] investigated the hydrogen storage properties and the reaction pathways of MgH_2–$NaAlH_4$ (4:1)/Na_3AlH_6 (4:1) composites. In this section, their results are compared with our thermodynamic calculations.

The calculated MgH_2–$NaAlH_4$ phase diagram is presented in Fig. 19 and shows the different reaction stages in the thermal decomposition of MgH_2/$NaAlH_4$ composites at 1 bar.

It can be seen that the reaction pathway in the MgH_2/$NaAlH_4$ composites depends on the relative amounts of the

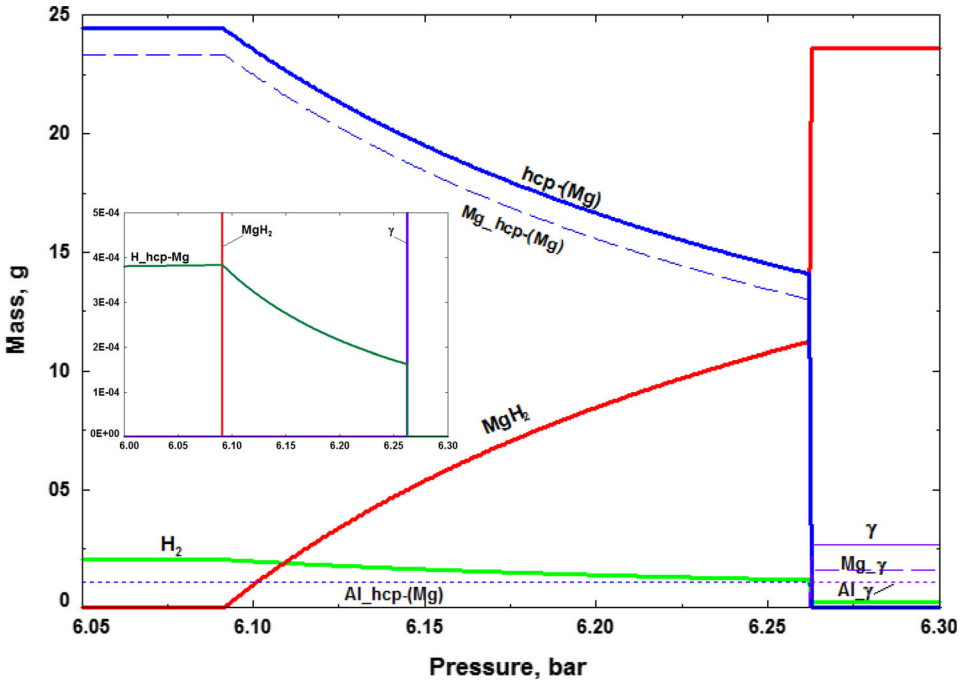

Fig. 18 Hydriding reaction path of Mg-4 at% Al at 350 °C

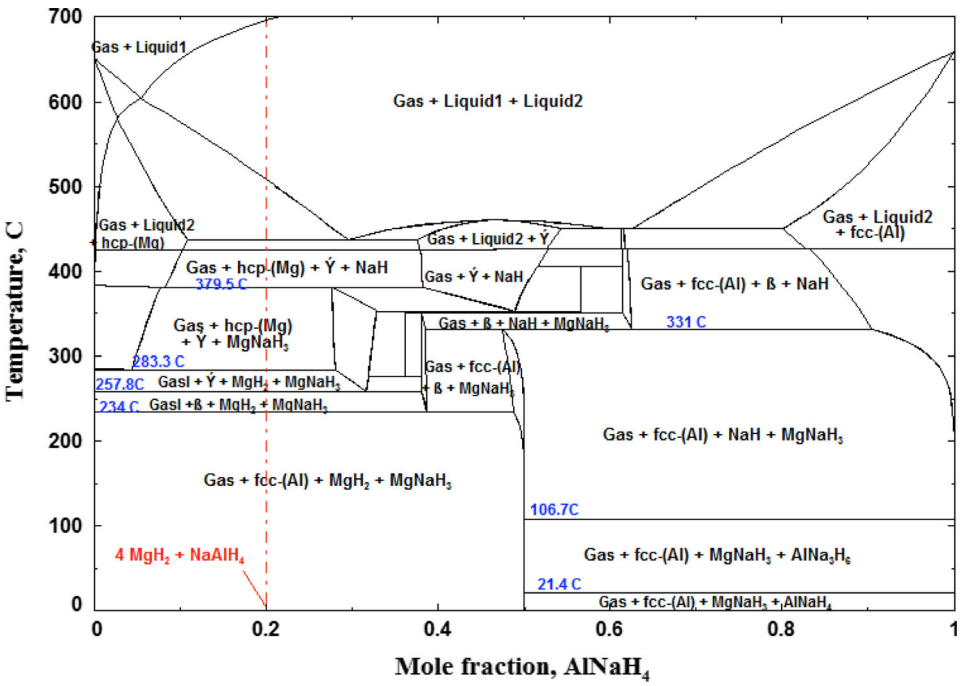

Fig. 19 The calculated MgH_2–$AlNaH_4$ phase diagram at 1 bar

components. For MgH_2–$NaAlH_4$ (4:1) composition (marked by red dashed line in Fig. 19), NaAlH4 reacts spontaneously with MgH_2 to form $NaMgH_3$, MgH_2, and fcc-Al. Then, as already discussed in "Al–Mg–H system", MgH_2 interacts with fcc-Al and decomposes in three steps: at 234 °C (when β is formed), at 257.86 °C (when γ is formed), and at 283.29 °C (when γ and hcp-Mg are formed). Finally, $NaMgH_3$ and NaH decompose at 379.48 and 424.8 °C, respectively. The (TPD) results [8] showed that four stages of $4MgH_2$–$NaAlH_4$-TiF_3 desorption have been observed in the temperature ranges (60–200 °C), (200–315 °C), (315–370 °C), and (after 375 °C), respectively.

The results of Ismail et al. [7, 8] are in agreement with the calculations performed in this work. However, the first stage desorption reported by Ismail et al. [7, 8] was attributed to the reaction between a part of MgH_2 and $NaAlH_4$ to form $NaMgH_3$ and Al. This reaction happens spontaneously according to our calculation and might be kinetically hindered. Ismail et al. [7, 8] reported the decomposition of MgH_2 as a one-step process and this might be due, in addition to kinetics factor, to the small differences in the three steps reaction temperatures (234, 257.8, and 283.29 °C, respectively) calculated in this work. In addition to that, the desorption temperatures reported [8] are in a good agreement with the calculated ones at 1 bar considering the fact that the TPD experiments were performed in vacuum [7, 8].

It should be noted that according to the calculation reported in Fig. 19 (the red dashed line for $4MgH_2 + NaAlH_3$ composition) and the results reported in "Al–Mg–H system" Fig. 12a (the red dashed line for $MgH_2 + 0.25AlH_3$ composition), $NaMgH_3$ does not affect the decomposition temperatures of MgH_2 + Al mixtures. However, the decomposition temperature of $NaMgH_3$ is decreased from 382.63 °C for pure $NaMgH_3$ [2] to 379.48 °C in the MgH_2–$NaAlH_4$ (4:1) composite.

Figure 19 shows the reaction processes in MgH_2–$NaAlH_4$ composites for the whole composition range. According to our calculations, it is predicted that for $NaAlH_4$ content above 0.5 mol fraction (in Fig. 19), MgH_2 decomposes spontaneously and the system is initially composed of fcc-Al, $MgNaH_3$, and $AlNaH_4$. The first and the second reaction steps concern the decomposition of $AlNaH_4$ and $AlNa_3H_6$ at the hydrides' decomposition temperatures, 21.4 and 106.7 °C, respectively, which shows that these hydrides are not altered by Al or $MgNaH_3$. Between 0.62 and 0.9 mol fractions of $NaAlH_4$, $NaMgH_3$ decomposes in one step at 331 °C. This temperature is 51.63 °C lower than the decomposition temperature of pure $NaMgH_3$. This fact proves that Al alters the decomposition process of $NaMgH_3$. The reaction pathway of $0.2Al + 0.8NaMgH_3$ composite is presented in Fig. 20. The Al and Mg content of each phase are presented in the enlarged inset with dotted and dashed lines, respectively, with the same color as the phase. It is shown that $MgNaH_3$ decomposes in four steps with the formation of β, $Al_{30}Mg_{23}$, γ, and hcp-Mg at 331, 350.27, 352.19, and 379.48 °C, respectively. In each step, NaH and H_2 are also formed. It should be noted that with increasing

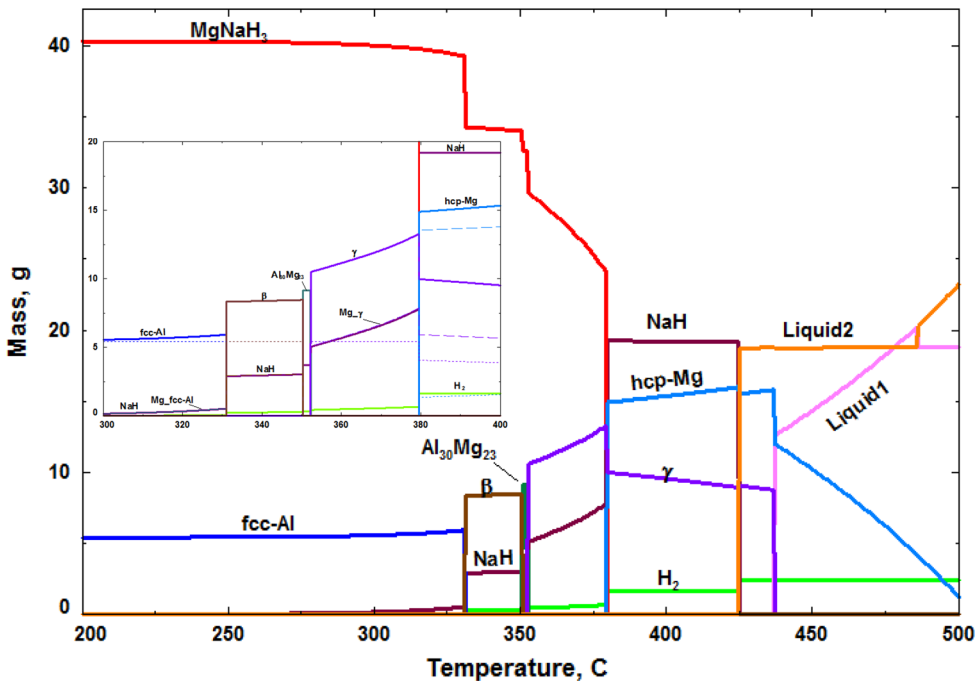

Fig. 20 Reaction path of the reaction 0.2 Al + 0.8 $NaMgH_3$ at 1 bar

temperature, Fig. 20 shows that the amount of $MgNaH_3$ starts decreasing at temperatures below 331 °C and that the amount of fcc-Al increases while its Al content is constant. The amount of NaH in the composite increases too. We can conclude that, when Al is added to $MgNaH_3$, some Mg starts dissolving in fcc-Al forming NaH and liberating some H_2 until fcc-Al saturation where β forms at 331 °C. The same conclusion can be drawn regarding Mg solubility in β and γ.

Ismail et al. [7] demonstrated that the reactions in MgH_2–$NaAlH_4$ (4:1) composite are reversible at 30 bar H_2 pressure and 300 °C, except the first one (reaction between MgH_2 and $NaAlH_4$ to form $NaMgH_3$ and Al), and that the phases present in the composite after rehydrogenation are MgH_2, $NaMgH_3$, and Al. The calculated PT diagram of MgH_2–$NaAlH_4$ (4:1) composites is shown in Fig. 21. It shows also that at 300 °C and 30 bar (marked in the Fig. 21 by blue point), the composite is composed of MgH_2, $NaMgH_3$, and fcc-Al phases, which agree with the results of Ismail et al. [7, 8]. In addition to these phases, Ismail et al. [7, 8] reported that XRD measurements showed a small peak of β phase in addition to Al_3Ti phase when TiF_3 was added to the mixture. Al_3Ti and TiF_3 act as catalysts to improve the desorption kinetics of the mixture [7, 8].

Ismail et al. [7, 8] showed that the absorption kinetics after the first desorption of the composite was slow compared to MgH_2 and that addition of TiF_3 did not improve it. This slow absorption kinetics has been related to the presence of β whose hydrogenation is kinetically hindered [7, 8].

It can be concluded from these calculations and the work of Ismail et al. [7, 8] that $NaAlH_4$ is destabilized by MgH_2 and decomposes spontaneously in the mixture MgH_2–$NaAlH_4$ (4:1). Then, the produced Al destabilizes MgH_2. But the re-hydrogenation reactions kinetics is very slow.

Ismail et al. [9] investigated the hydrogen storage properties of the MgH_2–Na_3AlH_6 (4:1) composite and concluded that the reaction mechanisms were similar to that of the MgH_2–$NaAlH_4$ (4:1) composite. The calculated MgH_2–Na_3AlH_6 phase diagram is presented in Fig. 22 and is very similar to the calculated MgH_2–$NaAlH_4$ phase diagram. A red dashed line in Fig. 22 shows the MgH_2–Na_3AlH_6 (4:1) composition. It shows that MgH_2 decomposes in two steps with the formation of β phase in the first step and γ with β phases after the second step. The present calculations show the formation of $Al_{30}Mg_{23}$, which has not been reported in the literature. Figure 22 shows that a small variation in the mixture composition will result in identical reaction mechanisms as with MgH_2–$NaAlH_4$ (4:1) composite. It might be the case in the results published by Ismail et al. [9].

The calculated PT diagram of MgH_2–Na_3AlH_6 (4:1) composites is shown in Fig. 23. It shows that Na_3AlH_6 is not stable in this mixture even under very high pressures. XRD results [9] showed that the rehydrogenated composite at 30 bar and 300 °C, was composed of MgH_2, $NaMgH_3$, Al, and a small amount of β which agrees with the calculations performed in this work (Fig. 23), except for the existence of β which shows that its hydrogenation process is very slow.

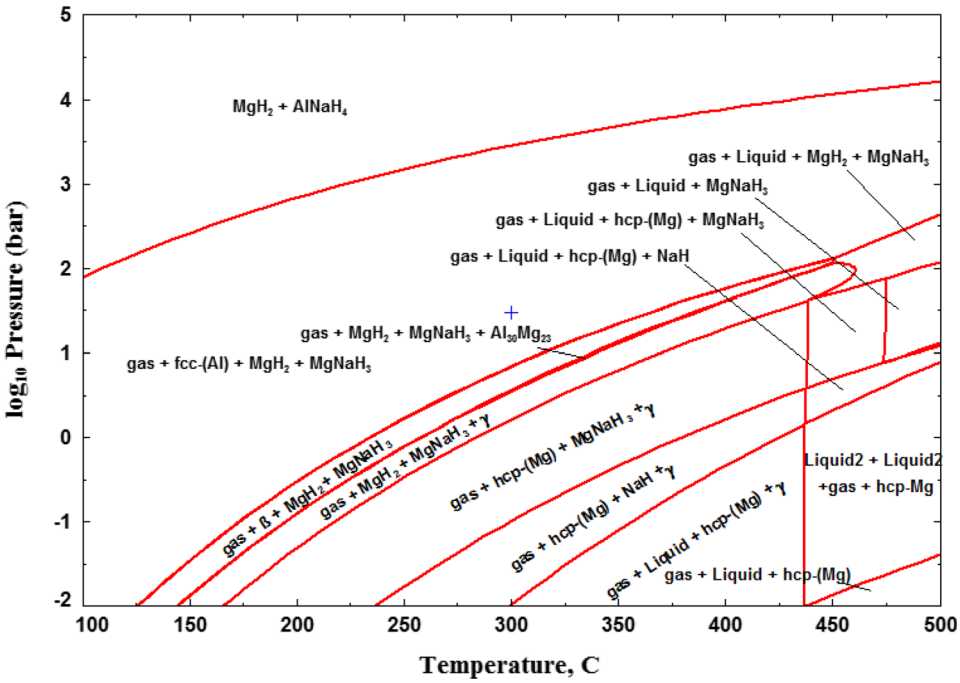

Fig. 21 P–T diagram of the $4MgH_2 + NaAlH_4$ composite

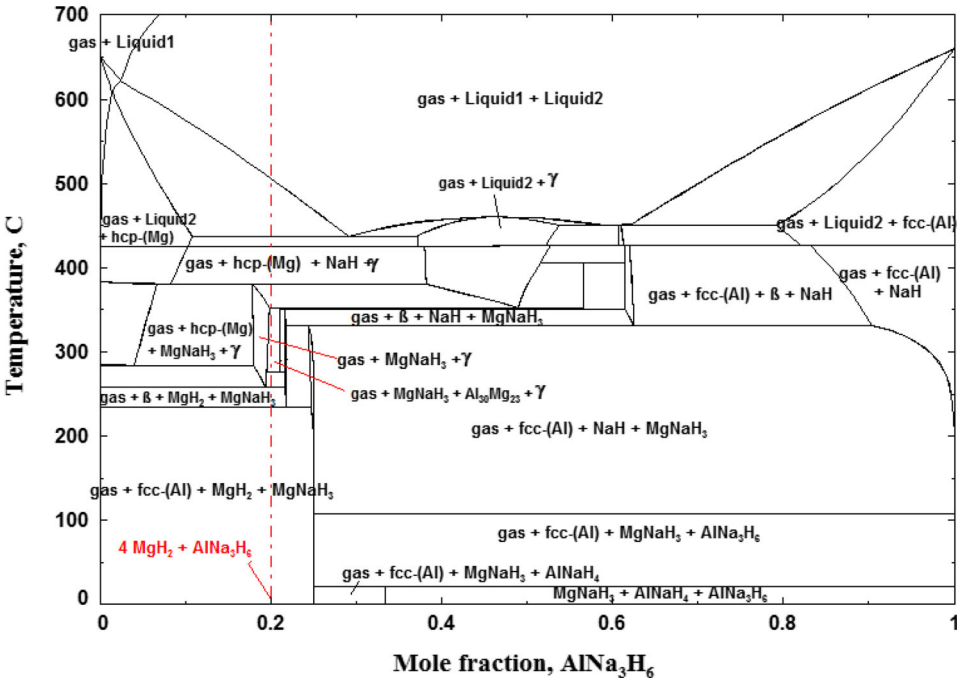

Fig. 22 The calculated MgH_2–$AlNa_3H_6$ phase diagram at 1 bar

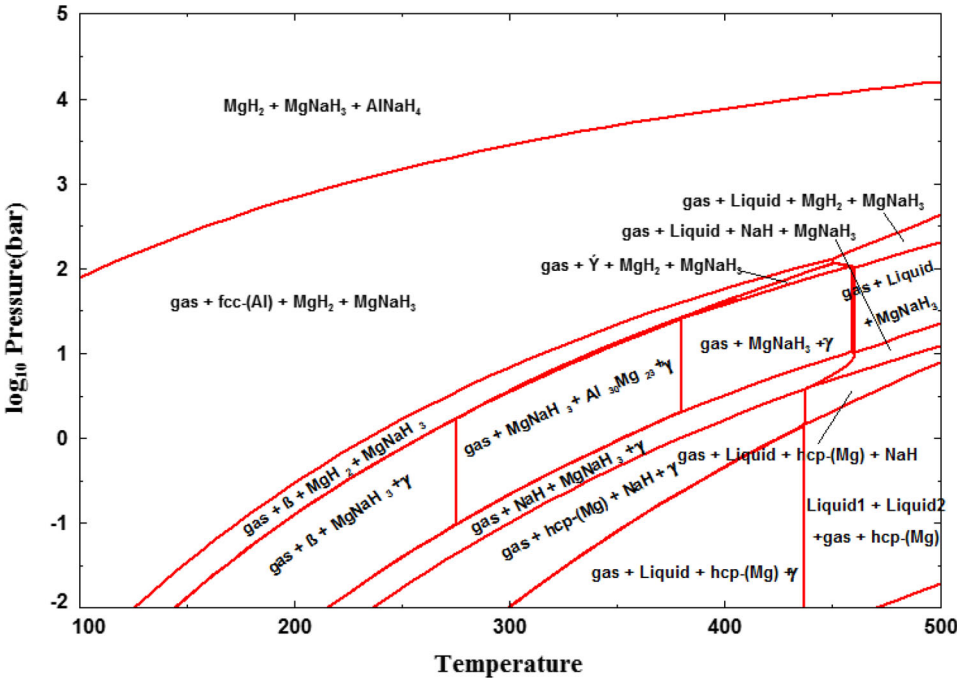

Fig. 23 P–T diagram of the $4MgH_2 + Na_3AlH_6$ composite

According to the thermodynamic calculations conducted in this work, at 1 bar, $AlNaH_4$ decomposes to form $AlNa_3H_6$ and fcc-Al at 21.4 °C, and $AlNa_3H_6$ decomposes to form NaH and fcc-Al at 106.7 °C. When mixed with MgH_2, $MgNaH_3$ forms spontaneously from MgH_2 and $AlNaH_4$/$AlNa_3H_6$ and the resulting mixture composition depends on the relative amounts of the components.

When the number of Mg atoms in $MgH_2 + AlNaH_4$/$AlNa_3H_6$ mixture exceeds the number of Na atoms, all the $AlNaH_4$/$AlNa_3H_6$ decomposes spontaneously and the remaining decomposition steps concern the decomposition of (MgH_2 + Al) mixture and $MgNaH_3$ has only a catalytic role.

When the number of Na atoms in the $MgH_2 + AlNaH_4$/$AlNa_3H_6$ mixture exceeds the number of Mg atoms, MgH_2

decomposes spontaneously and the remaining steps concern the decomposition of $AlNaH_4$ and $AlNa_3H_6$ which is not affected by $MgNaH_3$.

Ismail et al. [9] compared the hydrogen storage properties of $4MgH_2 + AlNaH_4$ and those of $4MgH_2 + AlNa_3H_6$ mixtures. The TPD curves [9] show that both composites start to decompose at around 170 °C, which is 10 and 55 °C lower than the decomposition temperature of the as-milled $AlNaH_4$ and $AlNa_3H_6$, respectively. For this reason, Ismail et al. [9] concluded that the $MgH_2 + AlNa_3H_6$ composite is better than the $MgH_2 + AlNaH_4$ composite. However, according to our calculations, there is no difference in the decomposition process of the two composites and the mutual destabilization of MgH_2 and $AlNaH_4/AlNa_3H_6$ hydrides in this composition range ($4MgH_2 + AlNa_3H_6$, when the number of Mg atoms exceeds the number of Na atoms) does not depend on the hydrides' decomposition temperatures.

Conclusion

In this work, thermodynamic modeling is used to investigate the reaction mechanisms and hydrogen storage properties in the Al–Mg–Na–H system. A self-consistent database has been constructed by extrapolating the different binaries assessed in this work or taken from the literature, using the CALPHAD method.

The reaction pathways for the reaction MgH_2/AlH_3, $MgH_2/NaAlH_4$, and MgH_2/Na_3AlH_6 are calculated and show good agreement with experimental data from the literature and provide insight regarding the reaction temperatures, the amount of the products, and their composition. It is shown that Al destabilizes MgH_2 by the formation of Al–Mg solid solutions and compounds. This process depends on Al content. The first step decomposition temperature of MgH_2 in the mixture at 1 bar is 234 °C; i.e., 50.73 °C lower than the decomposition temperature of MgH_2 alone and is due to the formation of the β phase. The calculated pressure–composition isotherms for Mg-10 at% Al and Mg-4 at% Al alloys at 350 °C show good agreement with the experimental data and give a more detailed description of the hydriding process products and equilibrium pressures. These calculations explain the uncertainties found in the literature, especially the sloping curves and difficult plateau pressures distinction. It is shown that the first hydrogenation of Al–Mg alloys starts at higher pressure than pure Mg and depends on the Al content. In fact, for Al content higher than 7 at%, the hydrogenation of hcp-Mg occurs in one step with the formation of the γ phase at 6.26 bar. However, for Al content lower than 7 at%, the hcp-Mg is hydrogenated first at pressures increasing with Al content (5.84 bar for pure Mg to 6.26 bar for 7 at% Al in Mg alloy) and is related to the solubility of Al in hcp-Mg, followed by the formation of the γ phase at 6.26 bar. It is shown that the PCIs sloping reported in the literature for the Al–Mg alloys is, in addition to kinetic factors, due to the large solubility of the γ phase, to short plateaus' length, and to the small differences between plateau pressures.

For $MgH_2/NaAlH_4$ and MgH_2/Na_3AlH_6, it is shown that reaction mechanisms in the composites depend on the relative amount of the components. It is demonstrated that each component of the composite destabilizes the other component in a specific composition range by the formation of $NaMgH_3$. When the number of Mg atoms in the $MgH_2 + AlNaH_4/AlNa_3H_6$ mixture exceeds the number of Na atoms, all the $AlNaH_4/AlNa_3H_6$ decomposes spontaneously and the remaining decomposition steps concern the decomposition of (MgH_2 + Al) mixture and $MgNaH_3$ acts only as a catalyst.

When the number of Na atoms in $MgH_2 + AlNaH_4/AlNa_3H_6$ mixture exceeds the number of Mg atoms, MgH_2 decomposes spontaneously and the remaining steps concern the decomposition of $AlNaH_4$ and $AlNa_3H_6$, which is not affected by $MgNaH_3$ that might have a catalytic effect on the process. $MgNaH_3$ in this mixture decomposes to form the β phase at 331 °C, i.e., 51.6 °C lower than the decomposition temperature of pure $MgNaH_3$.

References

1. Sakintuna, B., Lamari-Darkrim, F., Hirscher, M.: Metal hydride materials for solid hydrogen storage: a review. Int J Hydrog Energy **32**, 1121–1140 (2007)
2. Abdessameud, S., Mezbahul-Islam, M., Medraj, M.: Thermodynamic modeling of hydrogen storage capacity in Mg-Na alloys. Sci. World J. 2014, ID 190320 (2014). doi:10.1155/2014/190320
3. Bogdanović, B., Schwickardi, M.: Ti-doped alkali metal aluminium hydrides as potential novel reversible hydrogen storage materials. J. Alloys Compd. **253**, 1–9 (1997)
4. Qiu, C., Opalka, S.M., Olson, G.B., Anton, D.L.: Thermodynamic modeling of the sodium alanates and the Na–Al–H system. Zeitschrift Für Metallkunde **97**, 1484–1494 (2006)
5. Tanniru, M., Slattery, D.K., Ebrahimi, F.: A study of stability of MgH_2 in Mg–8 at% Al alloy powder. Int. J. Hydrog. Energy **35**, 3555–3564 (2010)
6. Tanniru, M., Slattery, D.K., Ebrahimi, F.: A study of phase transformations during the development of pressure-composition-isotherms for electrodeposited Mg–Al alloys. Int. J. Hydrogen Energy **36**(1), 639–647 (2011)
7. Ismail, M., Zhao, Y., Yu, X., Mao, J., Dou, S.: The hydrogen storage properties and reaction mechanism of the MgH_2–$NaAlH_4$ composite system. Int. J. Hydrogen Energy **36**, 9045–9050 (2011)

8. Ismail, M., Zhao, Y., Yu, X., Dou, S.: Improved hydrogen storage performance of MgH_2–$NaAlH_4$ composite by addition of TiF_3. Int. J. Hydrogen Energy **37**, 8395–8401 (2012)
9. Ismail, M., Zhao, Y., Dou, S.: An investigation on the hydrogen storage properties and reaction mechanism of the destabilized MgH_2-Na_3AlH_6 (4:1) system. Int. J. Hydrogen Energy **38**, 1478–1483 (2013)
10. Liu, H., Wang, X., Liu, Y., Dong, Z., Cao, G., Li, S., Yan, M.: Improved hydrogen storage properties of MgH_2 by ball milling with AlH_3: preparations, de/rehydriding properties, and reaction mechanisms. J. Mater. Chem. A **1**, 12527–12535 (2013)
11. Liu, H., Wang, X., Liu, Y., Dong, Z., Ge, H., Li, S., Yan, M.: Hydrogen desorption properties of the MgH_2–AlH_3 composites. J. Phys. Chem. C **118**, 37–45 (2014)
12. Bale, C., Pelton, A., Thompson, W.: FactSage 6.4, Factsage thermochemical software and databases (2013). http://www.crct.polymtl.ca/.
13. Qiu, C., Olson, G.B., Opalka, S.M., Anton, D.L.: Thermodynamic evaluation of the Al-H system. J. Phase Equilib. Diffus. **25**, 520–527 (2004)
14. Harvey, J.: Developpement d'une base de donnees thermodynamique pour la modelisation de la solubilite d'hydrogene dans les alliages d'aluminium. Thesis, Ecole Polytechnique, Montreal, Canada, M.Sc.A., (2007)
15. Harvey, J.P., Chartrand, P.: Modeling the hydrogen solubility in liquid aluminum alloys. Metall. Mater. Trans. B **41B**, 908–924 (2010)
16. San-Martin, A., Manchester, F.: The al-H (aluminum-hydrogen) system. J. Phase Equilib. **13**, 17–21 (1992)
17. Graetz, J., Reilly, J., Yartys, V., Maehlen, J., Bulychev, B., Antonov, V., Tarasov, B., Gabis, I.: Aluminum hydride as a hydrogen and energy storage material: past, present and future. J. Alloys Compd. **509**, S517–S528 (2011)
18. Murray, J.L.: The Al–Na (Aluminum-Sodium) system. J. Phase Equilib. **4**, 407–410 (1983)
19. Zhang, S., Han, Q., Liu, Z.: Thermodynamic modeling of the Al–Mg–Na system. J. Alloys Compd. **419**, 91–97 (2006)
20. Scheuber, E.: Study of the solubility of sodium in aluminum. Z. Metallkd. **27**, 83–85 (1935)
21. Fink, W., Willey, L., Stumpf, H.: Equilibrium relations in aluminum–sodium alloys of high purity. Trans AIME **175**, 364–371 (1948)
22. Ransley, C.E., Neufeld, H.: The solubility relationships in the aluminum–sodium and aluminum–silicon–sodium systems. J. Inst. Met. **78**, 25–46 (1950)
23. Hansen, S., Tuset, J., Haarberg, G.: Thermodynamics of liquid Al-Na alloys determined by using CaF_2 solid electrolyte. Metall. Mater. Trans. B **33**(4), 577–587 (2002)
24. Fellner, P., Korenko, M., Danielik, V., Thonstad, J.: The content of sodium in aluminium during electrolysis of the molten systems Na 3 AlF_6–NaCl–Al_2O_3 and NaF–NaCl. Electrochim. Acta **49**, 1505–1511 (2004)
25. Dewing, E.: Thermodynamics of system NaF-AlF_3. 3. Activities in liquid mixtures. Metall. Trans. **3**, 495–501 (1972)
26. Brisley, R., Fray, D.: Determination of the sodium activity in aluminum and aluminum silicon alloys using sodium beta alumina. Metall. Trans. B **14**, 435–440 (1983)
27. Rokhlin, L., Ivanchenko, V.: Al-H-Mg. In: Effenberg, G., Ilyenko, S. Effenberg, S.I.G. (eds.) Light metal ternary systems: phase diagrams, crystallographic and thermodynamic data, vol. 11A3, pp. 64–70. Springer-Verlag Berlin Heidelberg, Germany (2005)
28. Baukloh, W., Oesterlen, F.: The solubility of hydrogen in aluminum and some aluminum alloys. Z. Metallkd. **30**, 386–389 (1938)
29. Chernega, D.F., Gotvyanskii, Y.Y., Prisyazhnyuk, T.N.: Permeability, diffusion and solubility of H in Mg-Al alloys. Liteinoe Proizvod. **12**, 9–10 (1977)
30. Watanabe, T., Tachihara, Y., Huang, Y., Komatsu, R.: Effects of various alloying elements on the solubility of H in mg. J. Jpn. Inst. Light Metals **26**(4), 167–174 (1976)
31. Huang, Y.C., Watanabe, T., Komatsu, R.: Hydrogen in magnesium and its alloys. In: Proceedings of the 4th international conference on vacuum Metallurgy, pp. 176–179 (1974)
32. Øvrelid, E., Engh, T.A., Øymo, D.: vol. PA, pp. 771–78. Light Metals, TMS, Warrendale (1994)
33. Semenenko, K.N., Verbettskii, V.N., Kotchukov, A.V., Sytnikov, A.N.: Reaction of magnesium containing intermetallic compounds and alloys with hydrogen. Vestn. Mosk. Uni. Ser. 2 Khim **24**, 16–27 (1983)
34. Palumbo, M., Torres, F., Ares, J., Pisani, C., Fernandez, J., Baricco, M.: Thermodynamic and ab initio investigation of the Al–H–Mg system. Calphad **31**, 457–467 (2007)
35. Grove, H., Løvvik, O.M., Huang, W., Opalka, S.M., Heyn, R.H., Hauback, B.C.: Decomposition of lithium magnesium aluminum hydride. Int. J. Hydrog. Energy **36**, 7602–7611 (2011)
36. Mamatha, M., Bogdanović, B., Felderhoff, M., Pommerin, A., Schmidt, W., Schüth, F., Weidenthaler, C.: Mechanochemical preparation and investigation of properties of magnesium, calcium and lithium–magnesium alanates. J. Alloys Compd. **407**(1), 78–86 (2006)
37. Varin, R., Chiu, C., Czujko, T., Wronski, Z.: Mechano-chemical activation synthesis (MCAS) of nanocrystalline magnesium alanate hydride [mg $(AlH_4)_2$] and its hydrogen desorption properties. J. Alloys Compd. **439**(1), 302–311 (2007)
38. Kim, Y., Lee, E., Shim, J., Cho, Y.W., Yoon, K.B.: Mechanochemical synthesis and thermal decomposition of mg $(AlH_4)_2$. J. Alloys Compd. **422**(1), 283–287 (2006)
39. Iosub, V., Matsunaga, T., Tange, K., Ishikiriyama, M.: Direct synthesis of mg $(AlH_4)_2$ and $CaAlH_5$ crystalline compounds by ball milling and their potential as hydrogen storage materials. Int. J. Hydrog. Energy **34**(2), 906–912 (2009)
40. Sterlin Leo Hudson, M., Pukazhselvan, D., Irene Sheeja, G., Srivastava, O.: Studies on synthesis and dehydrogenation behavior of magnesium alanate and magnesium–sodium alanate mixture. Int. J. Hydrog. Energy **32**(18), 4933–4938 (2007)
41. Liu, Y., Pang, Y., Zhang, X., Zhou, Y., Gao, M., Pan, H.: Synthesis and hydrogen storage thermodynamics and kinetics of $Mg(AlH_4)_2$ submicron rods. Int. J. Hydrog. Energy **37**(23), 18148–18154 (2012)
42. Mintz, M., Gavra, Z., Kimmel, G., Hadari, Z.: The reaction of hydrogen with magnesium alloys and magnesium intermetallic compounds. J. Less Common Metals **74**(2), 263–270 (1980)
43. Gavra, Z., Hadari, Z., Mintz, M.: Effects of nickel and indium ternary additions on the hydrogenation of Mg-Al intermetallic compounds. J. Inorg. Nucl. Chem. **43**(8), 1763–1768 (1981)
44. Zaluska, A., Zaluski, L., Ström-Olsen, J.: Structure, catalysis and atomic reactions on the nano-scale: a systematic approach to metal hydrides for hydrogen storage. Appl. Phys. A **72**, 157–165 (2001)
45. Shang, C., Bououdina, M., Song, Y., Guo, Z.: Mechanical alloying and electronic simulations of (MgH_2-M) systems (M = Al, Ti, Fe, Ni, Cu and Nb) for hydrogen storage. Int. J. Hydrogen Energy **29**, 73–80 (2004)
46. Andreasen, A.: Hydrogenation properties of Mg–Al alloys. Int. J. Hydrogen Energy **33**, 7489–7497 (2008)
47. Nakamori, Y., Ninomiya, A., Kitahara, G., Aoki, M., Noritake, T., Miwa, K., Kojima, Y., Orimo, S.: Dehydriding reactions of mixed complex hydrides. J. Power Sour. **155**(2), 447–455 (2006)
48. Sartori, S., Qi, X., Eigen, N., Muller, J., Klassen, T., Dornheim, M., Hauback, B.C.: A search for new Mg- and K-containing

alanates for hydrogen storage. Int. J. Hydrogen Energy **34**(5), 4582–4586 (2009)
49. Dinsdale, A.T.: SGTE data for pure elements. Calphad **15**(4), 317–425 (1991)
50. Ransley, C., Talbot, D.: Hydrogen porosity in metals with special reference to aluminum and its alloys. Z. Metallkd. **46**(5), 328–337 (1955)
51. Hemmes, H., Driessen, A., Griessen, R.: Thermodynamic properties of hydrogen at pressures up to 1 Mbar and temperatures between 100 and 1000K. J. Phys. C Solid State Phys. **19**, 3571 (1986)
52. Dewing, E.W.: Thermodynamics of the system NaF-AlF_3: part VI. Revision. Metall. Trans. B **21**(2), 285–294 (1990)
53. Claudy, P., Bonnetot, B., Letoffe, J.: Preparation and physico-chemical properties of magnesium alanate. J. Therm. Anal. **15**, 119–128 (1979)
54. Bouaricha, S., Dodelet, J., Guay, D., Huot, J., Boily, S., Schulz, R.: Hydriding behavior of Mg–Al and leached Mg–Al compounds prepared by high-energy ball-milling. J. Alloys Compd. **297**(1), 282–293 (2000)